Chapter 5

Coupled Inductor Based Quadratic Gain Bidirectional DC-DC Converter

In this chapter, a coupled inductor based Quadratic gain bidirectional converter (QGBC) is described. This converter has only 4 power switches, 1 coupled inductor is used for the same voltage gain as QGBC. Therefore, the converter size and cost are reduced compared to the converter in chapter 4. The current ripple in coupled inductor based QGBC compared to QGBC, so the better system performance. As two inductor is replaced with a coupled inductor, the converter size and weight are also reduced. The coupled inductor reduced input current ripple in step-up and output current ripple in the step-down operation of the converter. The control technique of Voltage source inverter (VSI) in regenerative braking is different from that used in chapter 3.

5.1 Introduction

In the proposed converter, four switches with anti-parallel diodes, two capacitors, and a coupled inductor have been used. In comparison to conventional Bidirectional DC-DC converters (BDCs), the described non-isolated Bidirectional DC-DC converter (BDC) features a simple topology, control approach, and high voltage gain, ensuring wide voltage range operation. The proposed converter in this chapter is presented in Figure 5.1.
A brief outline of the chapter is as follows:

- Section 5.2 discusses the converter operation in step-up (motoring) mode for Continuous conduction mode (CCM) and Discontinuous conduction mode (DCM).

- Section 5.3 discusses the proposed converter operation in step-down (regenerative braking) mode for CCM and .DCM.

- The small-signal analysis of the converter is done in section 5.4.

- The simulation and prototype experimental validation of results are covered in section 5.5.

- The conclusion is given in section 5.6.

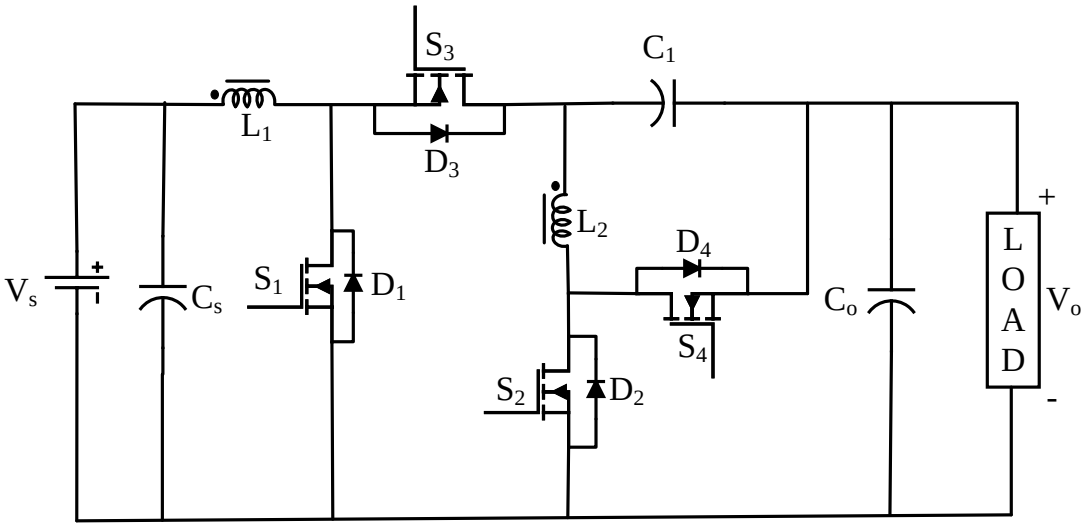

Figure 5.1: The topology of coupled inductor based QGBC.

5.2 Step-up or Motoring Operation

The suggested converter comprises of four switches S_1, S_2, S_3, and S_4 with anti-parallel diode, capacitor C_1, input and output capacitors C_s, C_o, and a coupled inductor with magnetising inductor L_m, leakage inductance L_1 and L_2 on the primary and secondary sides, respectively. On the low voltage side, a battery with voltage V_s is connected, and the DC link or output voltage is V_o. The proposed converter's operation is discussed in CCM and DCM.

5.2.1 Step-up in CCM

During step-up operation, the switches S_3 and S_4 are turned off, while the switches S_1, S_2 are controlled using a Pulse width modulation (PWM) technique. The step-up (motoring) operation of the converter can be explained by the following two modes. The woking waveform of the converter in step-up operation is shown in Figure 5.4.

Mode I (t_1, t_2): The switches S_1, S_2 are ON for time intervals 0 to DT_S, and S_3, S_4 are OFF. In this mode, the energy stored in the capacitor C_1 is transferred to the inductor L_2, so the current in inductor L_2 increases, the load is supplied through capacitor C_o, while inductor L_1 is being discharged due to negative voltage across it, and its current decreases. The current flowing path of the converter in this mode is shown in Figure 5.2.

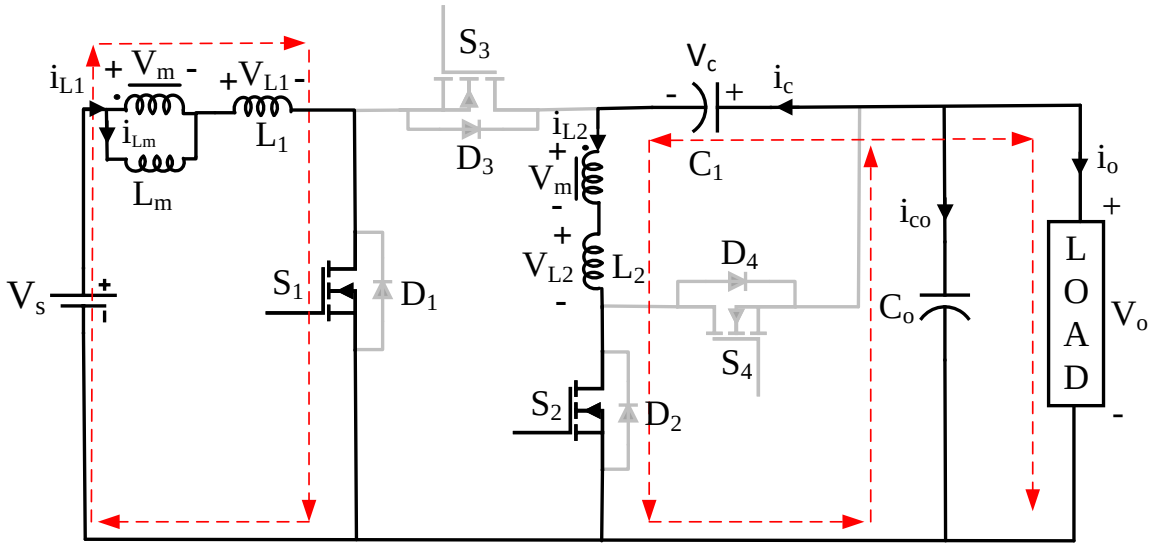

Figure 5.2: The current conduction path of the converter during mode I operation.

The voltage across inductor L_1,L_2 and current through capacitor C_1, C_o are obtained as follows:

$$V_{L1} = V_s - V_{mp} \tag{5.1}$$

$$V_{L2} = V_o - V_c - V_{ms} \tag{5.2}$$

$$i_c = i_{L2} \tag{5.3}$$

$$i_{co} = i_c + i_o \tag{5.4}$$

where the voltage across L_m in the primary and secondary sides of the coupled inductor is V_{mp}, V_{ms} respectively.

Mode II (t_2, t_3): In this mode, all the switches S_1, S_2 S_3, and S_4 are OFF, and the anti-parallel diode D_3 and D_4 are forward biased for a time interval (1-D)T_s. During this mode, the inductor L_2 is transferring its stored energy to the DC link capacitor C_o and load and capacitor C_1, inductor L_1 is charged by voltage source V_s. Figure 5.3 shows the conduction path during this mode of operation. The inductor current I_{L1} increases and inductor current I_{L2} decreases. The voltage across L_1, L_2 and current through capacitor C_1, C_o are obtained as follows:

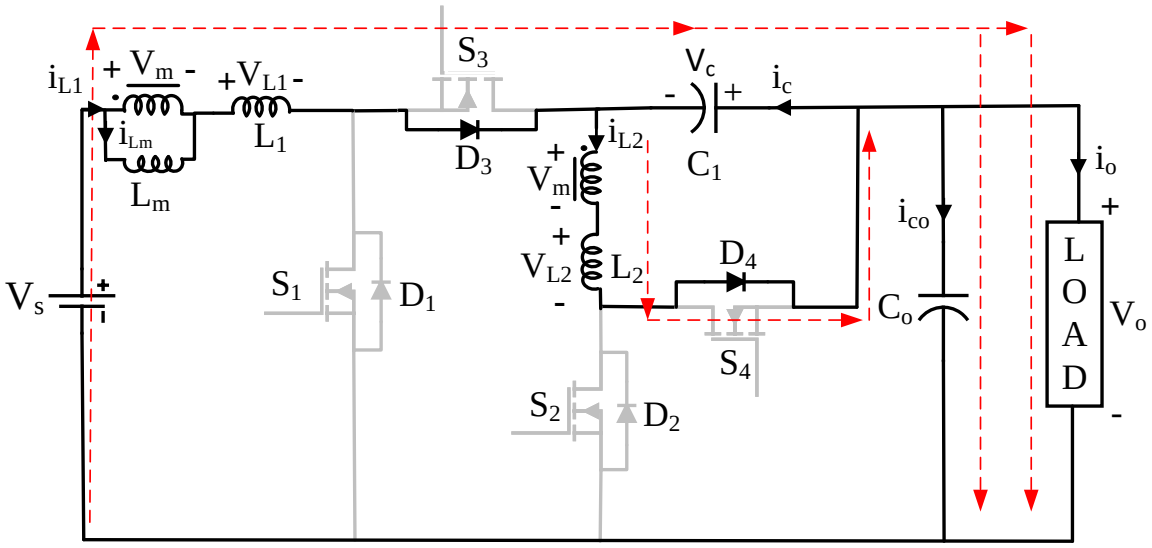

Figure 5.3: Current conduction path of the converter in mode II operation.

$$V_{L1} = V_s + V_c - V_{mp} - V_o \tag{5.5}$$

$$V_{L2} = -V_c - V_{ms} \tag{5.6}$$

$$i_c = -i_{L1} + i_{L2} \tag{5.7}$$

$$i_{co} = i_{L1} - i_o \tag{5.8}$$

Now applying the volt-sec balance principle across inductor L_1 and L_2 yields the following equations:

$$DV_s - DV_{mp} + (1-D)(V_s + V_c - V_{mp} - V_o) = 0 \tag{5.9}$$

$$DV_o - DV_c - DV_{ms} + (1-D)(-V_c - V_{ms}) = 0 \tag{5.10}$$

where D is the duty ratio, on solving (5.9) and (5.10) the voltage gain is obtained as

$$G_{step-up} = \frac{V_o}{V_s} = \frac{1}{(1-D)^2} \tag{5.11}$$

The voltage across capacitor C_1 is calculated as

$$V_c = \frac{V_s}{(1-D)} \tag{5.12}$$

From (5.11), the $G_{step-up}$ is independent of the turns ratio of the coupled inductor. So that the V_{mp} and V_{ms} are considered equal, and it is denoted as V_m.

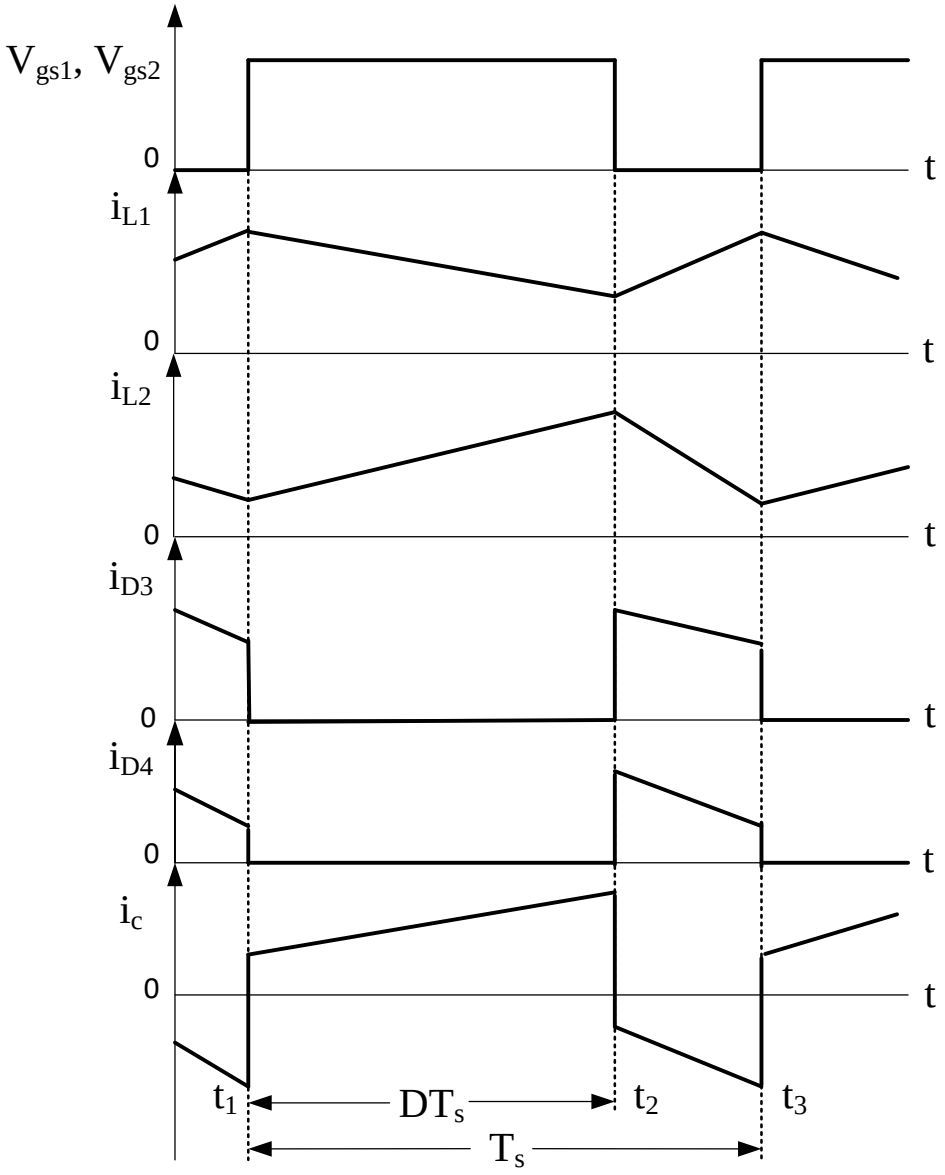

Figure 5.4: The working waveform of current and voltage of the converter during step-up operationi CCM.

After that, application of the ampere-sec balance principle on capacitor C_1 and C_o the following equation are obtained:

$$DI_{L2} + (1-D)(I_{L1} - I_{L2}) = 0 \tag{5.13}$$

$$DI_c + DI_o + (1-D)(I_{L1} - I_{L2}) = 0 \tag{5.14}$$

On solving the abovementioned equation, the average inductor current I_{L1} and I_{L2} are obtained:

$$I_{L1} = \frac{I_o}{(1-D)^2} \tag{5.15}$$

$$I_{L2} = \frac{I_o}{(1-D)} \tag{5.16}$$

Where I_o average load current in step-up operation. The load on the converter consists of a PMBLDC motor which is fed through a voltage source inverter. A pulley is connected to the shaft of the motor, load torque is applied on the pulley through the belt, both ends of the belt are connected with electronics weighing instrument.

The current ripples of the inductor are computed in time intervals t_1 to t_2 during step-up operation using the voltage equation across the inductor as shown in Figure 5.4

$$L_1\frac{di_{L1}}{dt} + L_m(\frac{di_{L1}}{dt} + \frac{di_{L2}}{dt}) = V_s \tag{5.17}$$

$$L_2\frac{di_{L2}}{dt} + L_m(\frac{di_{L1}}{dt} + \frac{di_{L2}}{dt}) = V_o - V_c \tag{5.18}$$

The ripple current in inductor L_1 is denoted as $\Delta\ i_{L1}$, inductor L_2 is denoted as $\Delta\ i_{L2}$ and dt=DT_s. Now solving (5.17) and (5.18) ripple current of inductors are obtained as

$$\Delta i_{L1} = \frac{V_s D T_s[L_2(1-D) - DL_m]}{L(1-D)} \tag{5.19}$$

$$\Delta i_{L2} = \frac{V_s D T_s[L_1 + DL_m]}{L(1-D)} \tag{5.20}$$

Where

$$L = L_1L_2 + L_1L_m + L_2L_m \tag{5.21}$$

5.2.2 Step-up in DCM

The proposed converter works in DCM when inductor L_2 current i_{L2} is discontinuous. The converter working voltage and current waveforms during DCM operation in step-up are presented in Figure 5.5.

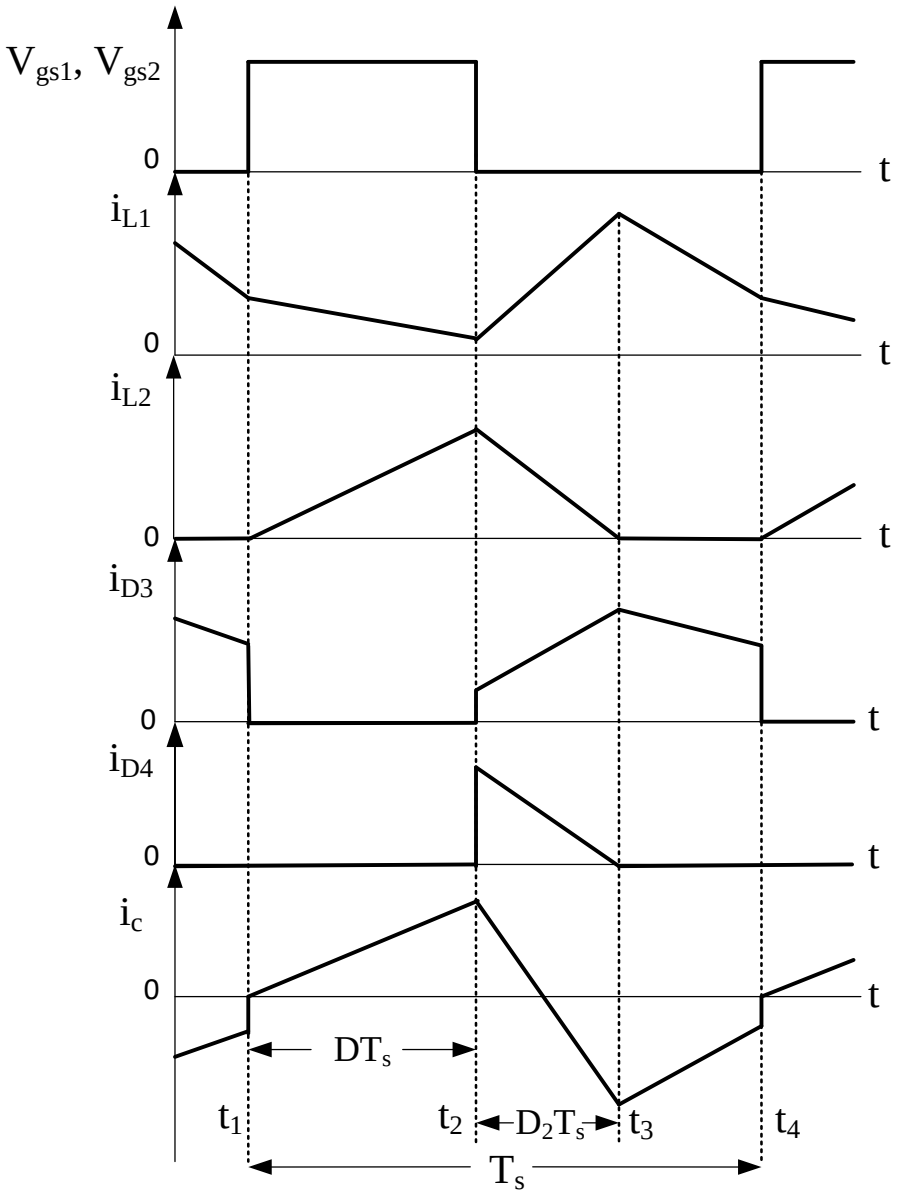

Figure 5.5: The working waveform of current and voltage of the converter during step-up operation in DCM.

Mode I (t_1, t_2): In this mode, the working of the converter is similar to Mode I of the CCM operation. The voltage across L_1, L_2, and current in capacitor C_1 and C_o are similar to the first mode of CCM.

Mode II (t_2, t_3): In this mode, S_1 and S_2 are turned OFF and anti-parallel diode D_3 and D_4 are in forward biased. The capacitor C_1 and inductor L_2 are discharged to the load and also capacitor C_o charged. The current through inductor L_1 is increased because the voltage across it is positive. The voltage across inductor L_1, L_2 and current through

capacitor C_1, C_o are written as

$$V_{L1} = V_o + V_c + V_s - V_{mp} \tag{5.22}$$

$$V_{L2} = -V_{ms} - V_c \tag{5.23}$$

$$i_c = i_{L2} - i_{L1} \tag{5.24}$$

$$i_{co} = i_{L1} - i_o \tag{5.25}$$

Mode III (t_3, t_4): In this mode, switches S_1 and S_2 are remains in OFF state. The anti-parallel diode D_4 is switched OFF since the inductor L_2 current is zero, while the anti-parallel diode D_3 remains turned ON and the inductor L_1 current is flowing. The inductor L_1 is discharged into the capacitor C_1 in this mode. The Figure 5.6 shows the current conduction path during this mode of operation. In this mode, capacitor C_o supplies the load because the inductor L_2 current is zero.

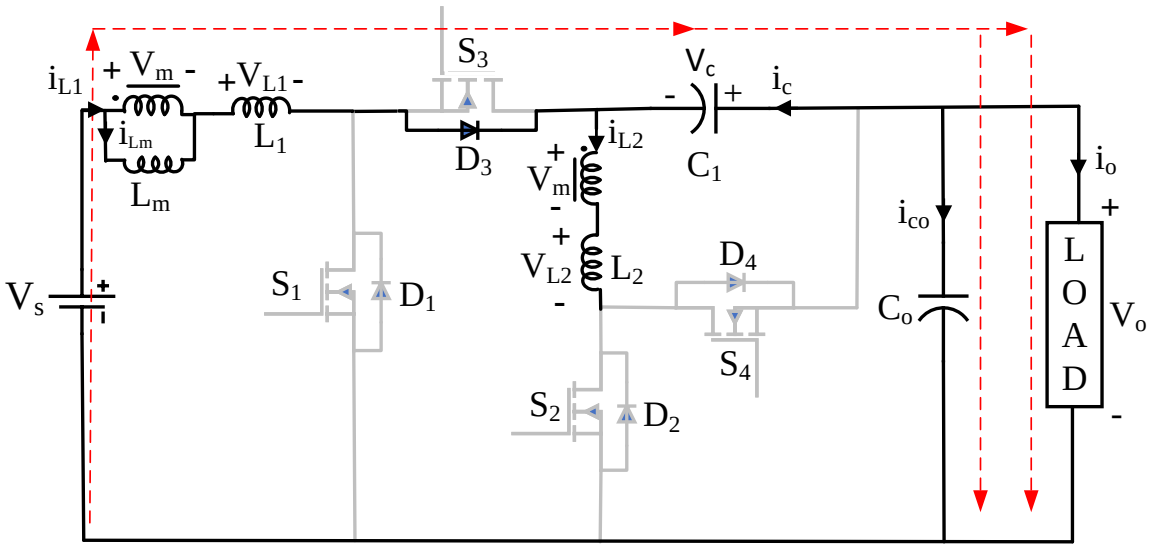

Figure 5.6: The current conduction path of the converter during step-up in mode III operation.

The current through capacitor C_1, C_o and the voltage across inductors L_1 and L_2, are written as

$$V_{L1} = V_o + V_c + V_s - V_{mp} \tag{5.26}$$

$$V_{L2} = 0 \tag{5.27}$$

$$i_c = -i_{L1} \tag{5.28}$$

$$i_{co} = i_{L1} - i_o \tag{5.29}$$

As the average current of D_4 is equal to I_o, substituting (5.19) into (5.17). Then the voltage gain of the converter in DCM is obtained as

$$\frac{V_o}{V_s} = \frac{D[D_1 L(1-D) - DL_2(L_1+L_m)(1-D) - D^2 L_m(L_1+L_m)]}{KL(1-D)} \tag{5.30}$$

Where

$$K = \frac{2L}{R_o T_s} \tag{5.31}$$

Where D_1 is the duty ratio in mode II in DCM and it can be calculated by equalizing (5.20) equal to amount of $\Delta\ i_{L1}$ in mode II.

$$\frac{D_1 T_s(V_o - V_c)}{L_2} = \frac{V_s D T_s(L_1 + DL_m)}{L(1-D)} \tag{5.32}$$

After solving (5.32), the duty ratio D_1 is obtained as

$$D_1 = \frac{L_2(L_1 + DL_m)}{L} \tag{5.33}$$

According to the basic principle, if $\Delta\ i_{Lm} = 0$, then inducted voltage is zero and the converter will not work. So that, there should be minimum ripple current by selecting a proper value of inductors. The ripple current in magnetizing inductor L_m is the sum of ripple current in L_1 and L_2, therefore the ripple current is obtained as

$$\Delta i_{Lm} = \Delta i_s = \Delta i_{L1} + \Delta i_{L2} \tag{5.34}$$

$$L_m = \frac{V_s D T_s[L_1 + L_2(1-D)] - L_1 L_2(1-D)\Delta i_s}{\Delta i_s(1-D)(L_1+L_2)} \tag{5.35}$$

The inductor values can be selected as per the permissible current's ripple in (5.19), (5.20), and (5.35). Because getting the exact leakage inductances L_1 and L_2 are difficult, auxiliary inductors are connected in a series of either side of the coupled inductor to get calculated current ripple.

5.3 Step-down or Regenerative braking Operation

A reversal of energy flow is required for Regenerative braking (RB) operation. The PMBLDC motor should be used as a generator to reverse the energy flow. With the help of a bidirectional converter, the stored energy in the inertial flywheel is transferred back to the battery by stepping down the output voltage to the source voltage label.

5.3.1 Step-down in CCM

The switches S_1, S_2 are turned off during step-down or RB operation of the converter, and S_3, S_4 are regulated using the PWM technique. The step-down or RB operation of the converter is explained in the following two modes. The working waveform the current and voltage during step-down in CCM operation are illustrated in Figure 5.9.

Mode 1 (t_1, t_2): In this mode, the switches S_3, S_4 are ON, and the remaining two switches are OFF for the time of DT_s. The inductor L_2 and capacitor C_1 are energized through source voltage Vs. The inductor L_1 is supplied to the load and capacitor C_s. The current in inductor L_1 decreases and inductor L_2 current increases. The current conduction path of the converter in this mode is shown in Figure 5.7.

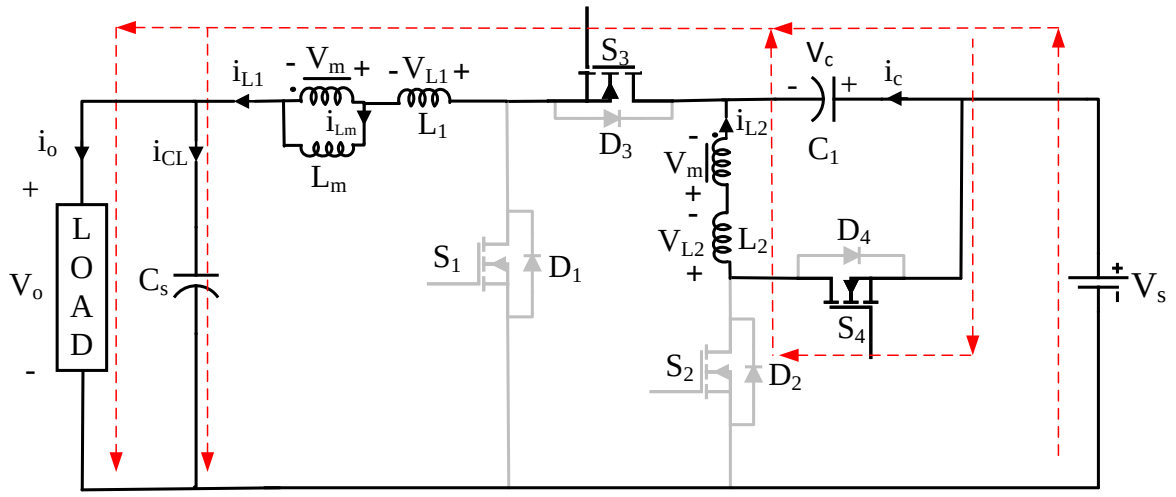

Figure 5.7: Current conduction path of the converter during step-down in mode I operation.

The voltage across L_1, L_2 and current through capacitor C_1, C_s are obtained as follows:

$$V_{L1} = V_s - V_c - V_{mp} - V_o \tag{5.36}$$

$$V_{L2} = V_c - V_{ms} \tag{5.37}$$

$$i_c = i_{L1} - i_{L2} \tag{5.38}$$

$$i_{cs} = i_{L1} - i_o \tag{5.39}$$

The amount of voltage generated in the primary and secondary sides of the coupled inductor is represented by V_{mp}, V_{ms}.

Mode II (t_2, t_3): All of the switches S_1, S_2, S_3, and S_4 are turned OFF. The anti-parallel diodes D_1 and D_2 are forward biased for a time period of (1-D)T_s. The energy stored in inductor L_2 is transferred to capacitor C_1, the load is provided by capacitor C_s, and inductor L_1 is charged due to positive voltage across it during this mode. The current conduction path of the converter during this mode is illustrated in Figure 5.8.

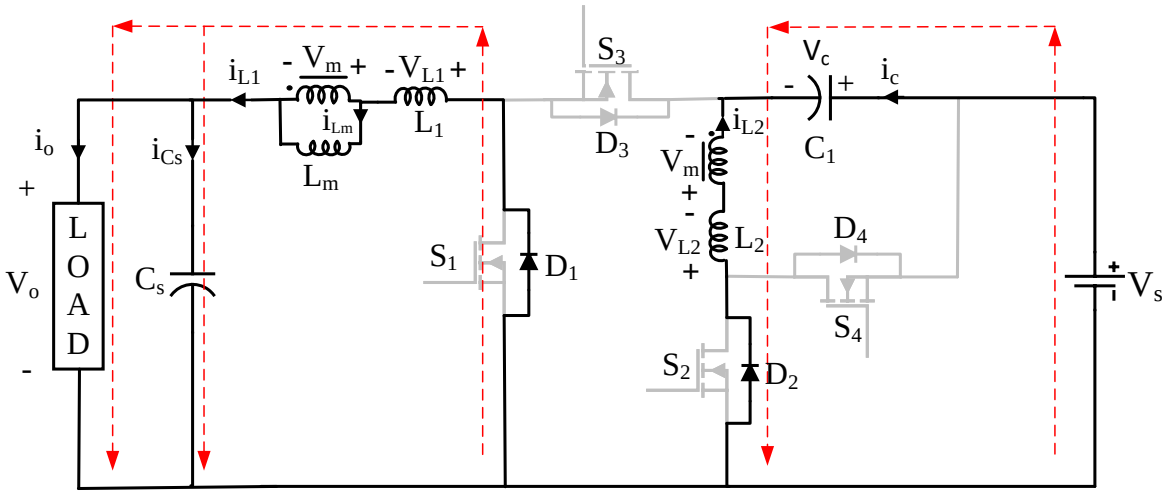

Figure 5.8: Current conduction path of the converter during step-down in mode II operation.

The voltage across L_1, L_2 and current through capacitor C_1, C_s are obtained as follows:

$$V_{L1} = V_o - V_{mp} \tag{5.40}$$

$$V_{L2} = V_c - V_s - V_{ms} \tag{5.41}$$

$$i_c = -i_{L2} \tag{5.42}$$

$$i_{cs} = i_{L1} - i_o \tag{5.43}$$

Now applying volt-sec balance principle on inductor L_1 and L_2 yields the following equation:

$$D(V_s - V_c - V_{mp} - V_o) + (1 - D)(V_o - V_{mp}) = 0 \tag{5.44}$$

$$D(V_c - V_{ms}) + (1 - D)(V_c - V_s - V_{ms}) = 0 \tag{5.45}$$

On solving (5.44) and (5.45), the voltage gain in step-down operation is obtained as:

$$G_{step-down} = \frac{V_o}{V_s} = D^2 \tag{5.46}$$

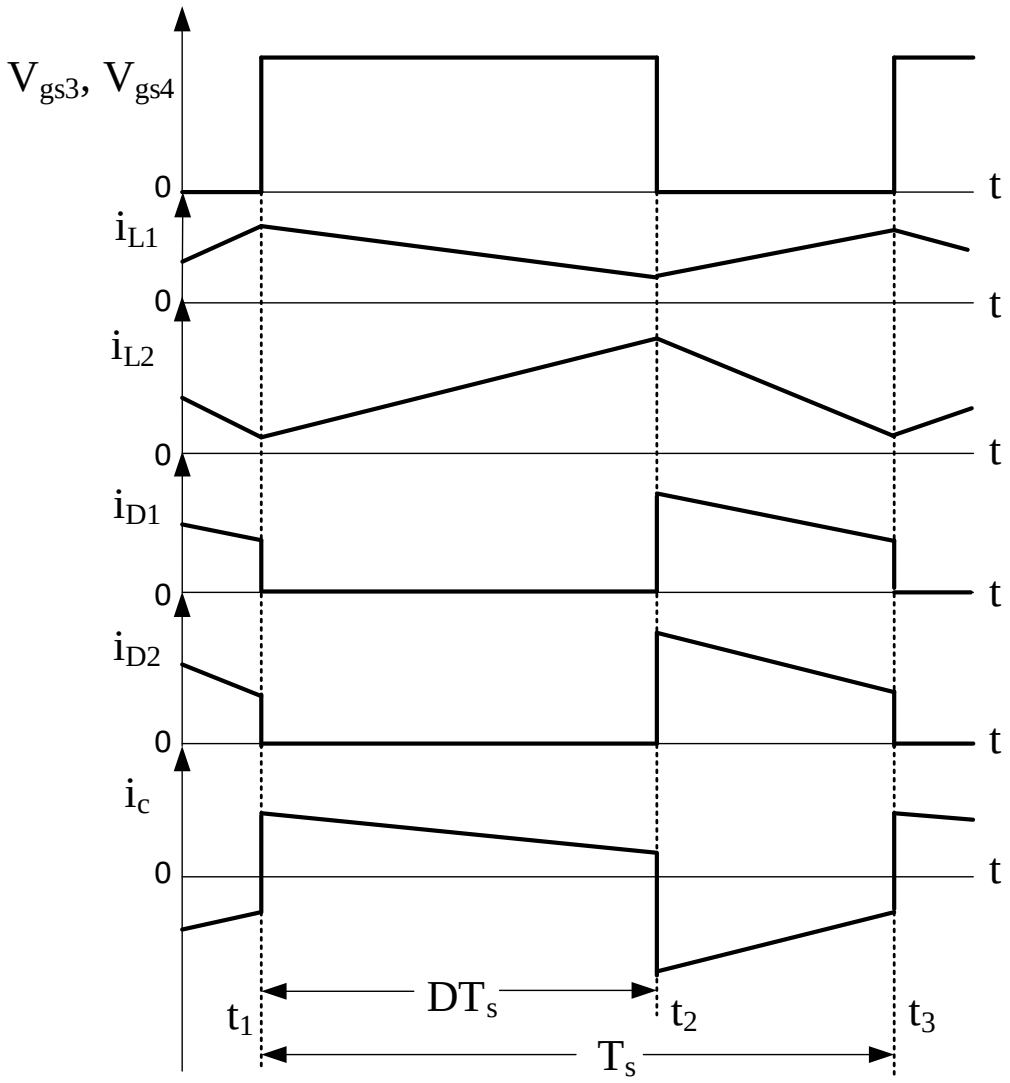

Figure 5.9: The working current and voltage waveform of the converter during step-down in CCM operation.

The voltage across capacitor C_1 is calculated as

$$V_c = DV_s \tag{5.47}$$

From (5.46), voltage gain $G_{step-down}$ is independent of the turns ratio of the coupled inductor. So that the V_{mp} and V_{ms} are considered equal, and it is denoted as V_m. Similarly, the ampere-sec balance principle on capacitor C_1 and C_s yields following equation:

$$D(I_{L1} - I_{L2}) - (1 - D)I_{L2} = 0 \tag{5.48}$$

$$DI_{L1} + DI_o + (1 - D)(I_o - I_{L1}) = 0 \tag{5.49}$$

On solving (5.48) and (5.49), the average inductor I_{L1} and I_{L2} are obtained as

$$I_{L1} = DI_o \tag{5.50}$$

$$I_{L2} = D^2 I_o \tag{5.51}$$

From Figure 5.9, the current ripples of the inductor are calculated by applying voltage equation across the inductor in time interval t_1 to t_2 of step-down operation as follows:

$$L_1 \frac{di_{L1}}{dt} + L_m(\frac{di_{L1}}{dt} + \frac{di_{L2}}{dt}) = V_s - V_c - V_o \tag{5.52}$$

$$L_2 \frac{di_{L2}}{dt} + L_m(\frac{di_{L1}}{dt} + \frac{di_{L2}}{dt}) = V_c \tag{5.53}$$

The ripple current in inductor L_1 is denoted as $\Delta\ i_{L1}$, inductor L_2 is denoted as $\Delta\ i_{L2}$ and dt=DT_s. On solving (5.52) and (5.53) the ripple current in inductors are obtained as

$$\Delta i_{L1} = \frac{V_s D T_s[L_2(1 - D - D^2) - L_m(1 - D)^2]}{L} \tag{5.54}$$

$$\Delta i_{L2} = \frac{V_s D T_s[L_1 - D L_m(1 - D)]}{L} \tag{5.55}$$

5.3.2 Step-down in DCM

The converter operates in DCM mode, when the inductor L_2 current is discontinuous. In DCM, the converter's typical current and voltage waveforms are shown in Figure 5.10.

Mode I (t_1, t_2): The converter operation in this mode is similar to Mode I step-down in CCM.

Mode II (t_2, t_3): For time interval $D_1 T_s$, the switches S_3 and S_4 are turned off, and the anti-parallel diodes D_1 and D_2 are forward biased. The energy stored in inductor L_2 is transferred to capacitor C_1 in this mode, while inductor L_1 is charged due to the positive voltage applied across it.

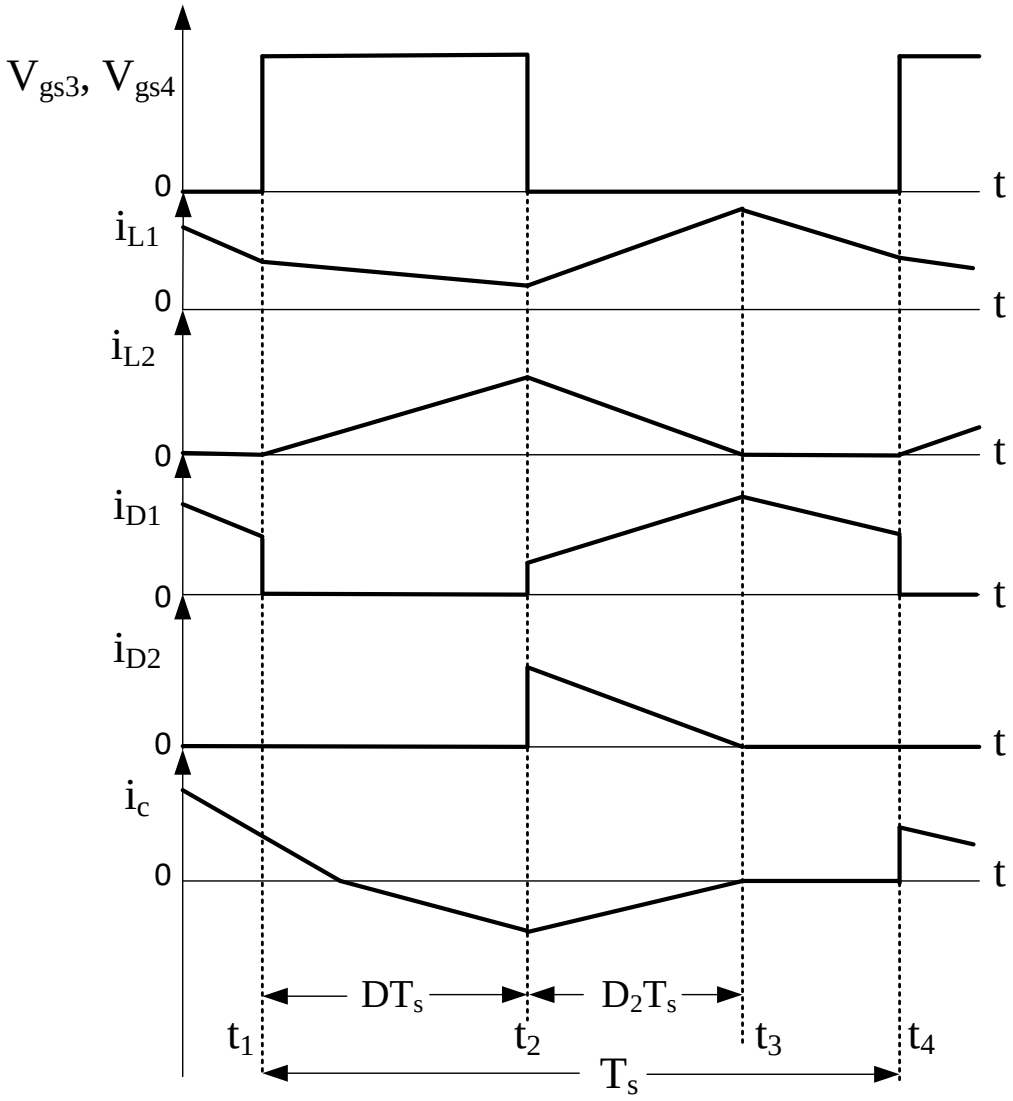

Figure 5.10: The working current and voltage waveform of the converter during step-down in DCM operation.

Mode III (t_3, t_4): The switches S_3 and S_4 are still switched OFF in this mode. The inductor L_2 current is zero, diode D_2 is turned OFF while diode D_1 is still ON, resulting in a continuous inductor L_1 current. The current conduction path in this mode is depicted in Figure 5.11. The voltage across inductors L_1, L_2 and the current in capacitors C_1, C_S are written as

$$V_{L1} = -(V_m + V_o) \tag{5.56}$$

$$i_{cs} = i_{L1} - i_o \tag{5.57}$$

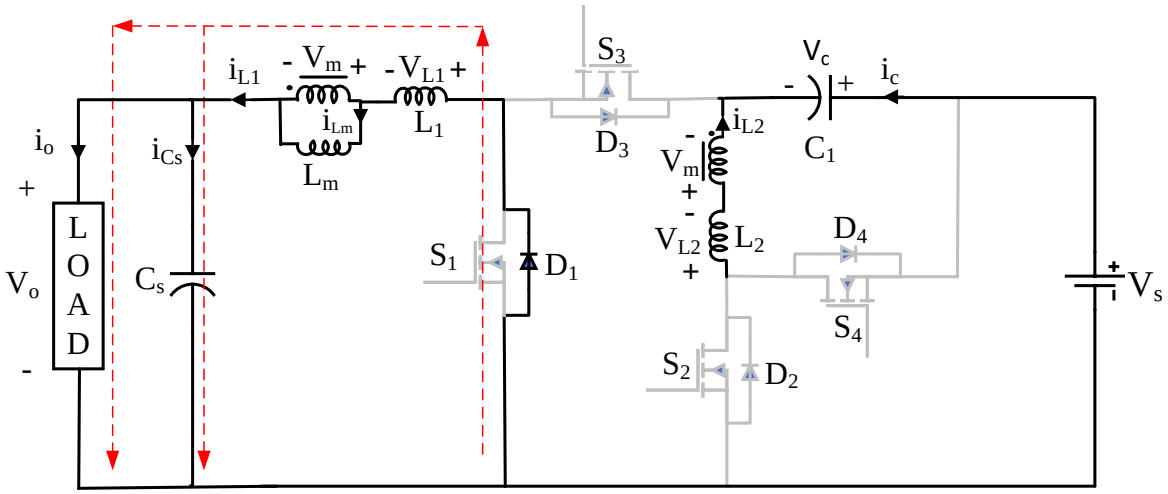

Figure 5.11: The current flowing path of the converter during step-down in mode III of DCM operation.

The average current of D_1 (I_{D1}) is equal to the average input current, V_{L2} is computed in Mode II by substituting (5.55) into (5.53), and the voltage gain in DCM is derived as

$$\frac{V_o}{V_s} = \frac{D_1^2[(L_1 + L_m)(1 - D)]}{KD^2 + D_1^2} \tag{5.58}$$

where

$$K = \frac{2L}{R_o T_s} \tag{5.59}$$

The duty D_1 in mode II as shown in Figure 5.10 can be calculated by equalizing (5.55) equal to the amount of $\Delta\, i_{L2}$ in mode II.

$$\frac{D_1 T_s(V_c - V_s}{L_2} = \frac{V_s D T_s[L_1 - DL_m(1 - D)]}{L} \tag{5.60}$$

After solving (5.60), the duty D_1 is obtained as

$$D_1 = \frac{L_1[L_2 + DL_m(L_1 + L_m)]}{L} \tag{5.61}$$

The output ripple current is equal to the sum of the ripple currents in inductor L_1 and L_2, which is equal to the ripple current in the magnetising current.

$$\Delta i_{Lm} = \Delta i_o = \Delta i_{L1} + \Delta i_{L2} \tag{5.62}$$

$$L_m = \frac{L_1 + L_2(1 - D - D^2) - L_m(1 - D)[DL_m + (1 - D)] - L_1 L_2 \Delta i_o}{\Delta i_o(L_1 + L_2)} \tag{5.63}$$

Therefore, the inductor's values are selected according to the permissible current ripple in (5.54), (5.55), and (5.63).

5.3.3 Regenerative braking commutation by single-switch strategy

The motor acts as a generator and kinetic energy is transferred to the battery during RB, which is accomplished by reversing power flow in the circuit with an appropriate switching method. A physical switch is used to change the mode of operation from motoring to regenerative braking and vice-versa. Back-Electromotive force (EMF) is insufficient to maintain battery voltage at the low speed of the PMBLDC motor. As a result, energy recovery is not possible. With the help of the motor's self-inductance, the back-EMF voltage must be raised to dc bus voltage to achieve energy recovery. Figure 5.12 shows the QGBC and VSI with equivalent circuit of a PMBLDC motor. The PMBLDC

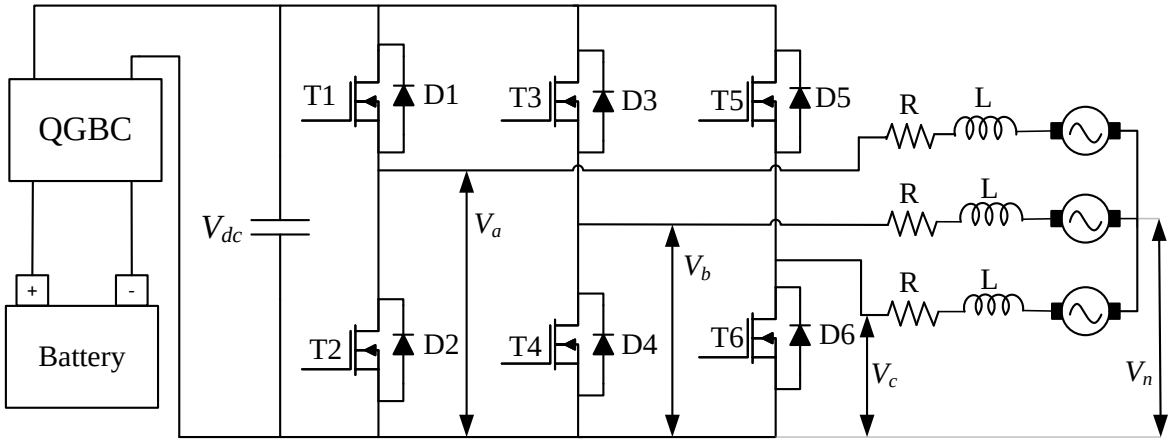

Figure 5.12: Bidirectional DC-DC converter and VSI with equivalent circuit of a PMBLDC motor.

motor armature current, back-EMF, and switching PWM of VSI are illustrated in Figure 5.13. In the single-switch strategy, power switches T2, T4 and T6 are operated in PWM switching mode and only one power switch is active during each commutation cycle. The power switches on the upper side of VSI are always off during the single-switch strategy. The switching PWM for the switches on the lower side of VSI is controlled based on the signal received from the hall sensor. Figure 5.14 shows the equivalent circuit of PMBLDC motor when PWM is given to power switch T2. At the instant the current in phase A is outgoing and current in phase B is incoming and switching PWM is given to switch T2. When switch T2 is turned ON, the back-EMF is utilized to built up armature current to generate electric braking torque whereas the electrical energy is stored in self-inductance

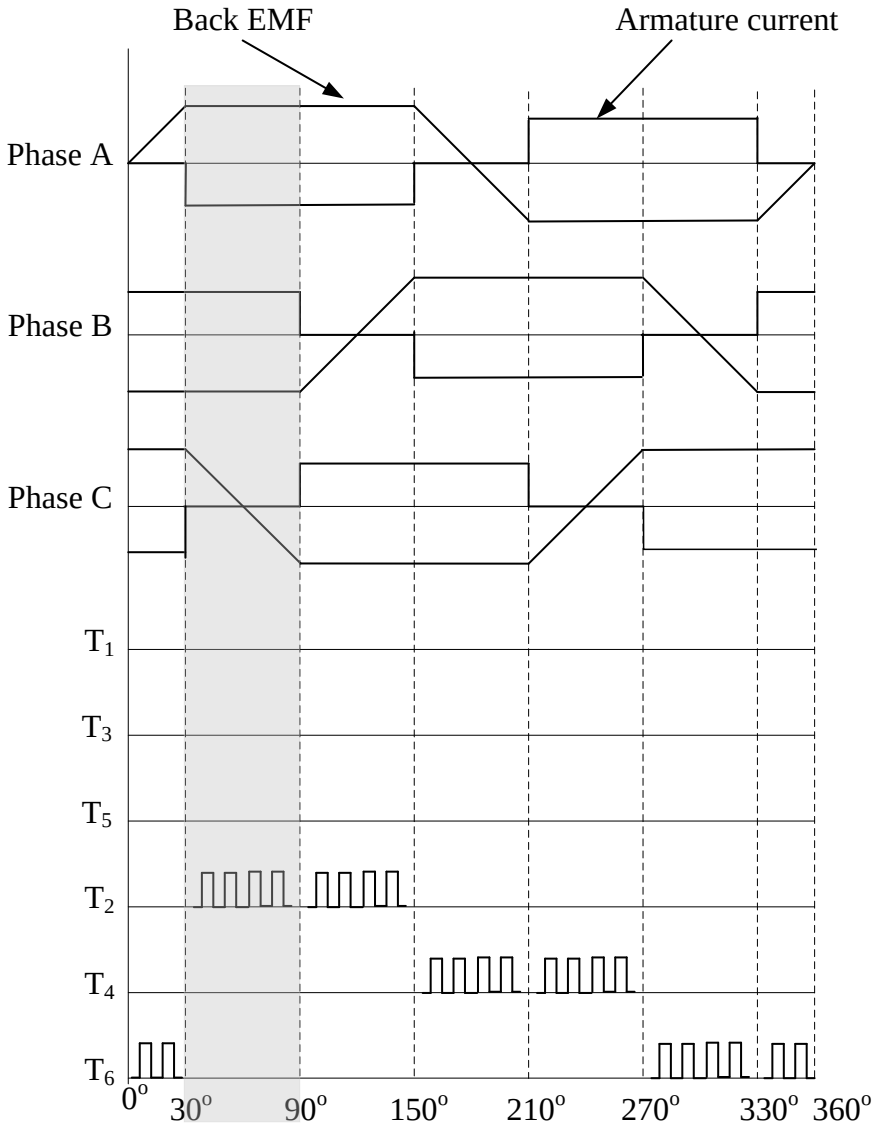

Figure 5.13: Back-EMF and armature current of PMBLDC motor with the switching signal for single-switch strategy.

of the motor. In contrast, when switch T4 is turned OFF, the energy stored in self-inductance is transferred to the battery through the freewheeling diode of T4. Suppose that the circuits are operating in steady-state continuous current conduction mode and all switches are ideal. Now applying volt-second and charge-second principle across inductor L and dc link capacitor respectively, the following equations are obtained:

$$\int_t^{t+T} v_L \, dt = \delta T[2V_{emf} - i_a(2R)] + \delta^{'} T[2V_{emf} - i_a(2R) - V_{dc}] = 0 \tag{5.64}$$

$$\int_t^{t+T} i_{dc} \, dt = \delta T(\frac{-V_{dc}}{R_e}) + \delta^{'} T(i_a - \frac{V_{dc}}{R_e}) = 0 \tag{5.65}$$

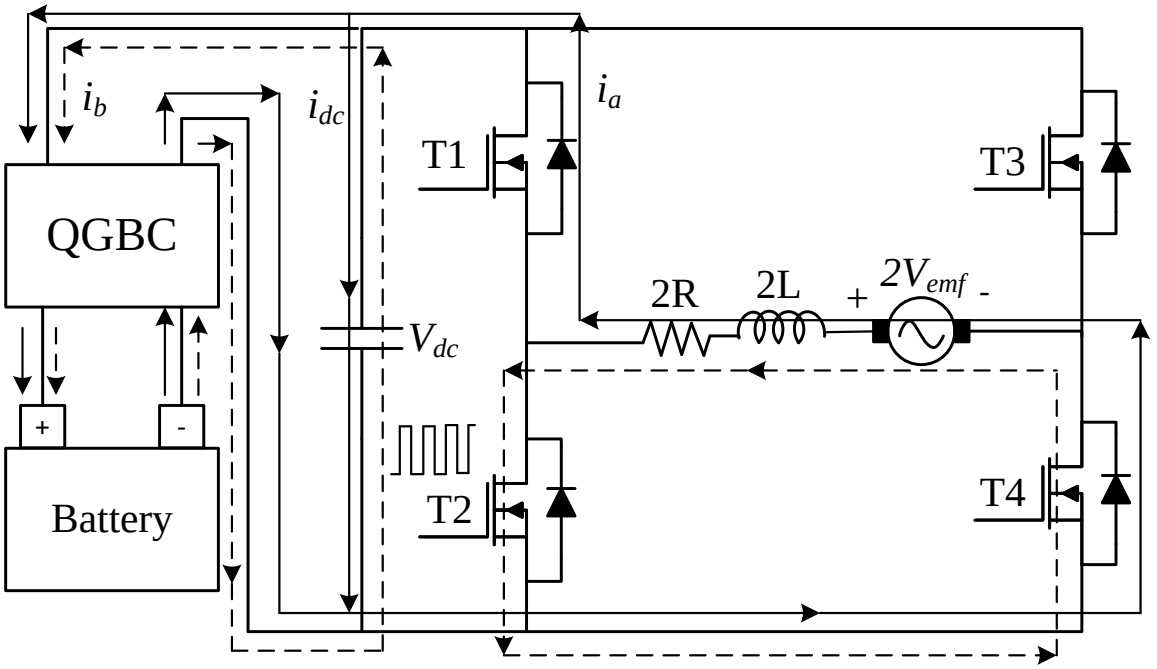

Figure 5.14: Current flowing path of single-switch control (solid line: OFF state; dotted line: On state).

where T is the switching period, $2V_{emf}$ is the back-EMF (e_a $+e_b$), R_e equivalent load resistance, R is armature winding resistance, δ is duty cycle, $\delta + \delta^{'}$=1, and i_a is the average armature current. On solving above two equation armature current and dc link voltage is obtained as:

$$i_a = \frac{2V_{emf}}{\delta'^2 R_e + 2R} \tag{5.66}$$

$$V_{dc} = \frac{2V_{emf}}{(\delta' + (2K/\delta'))} \tag{5.67}$$

where K is defined as R/R_e. The voltage boost ratio is derived as

$$\frac{V_{dc}}{V_{emf}} = \frac{2V}{(\delta' + (2K/\delta'))} \tag{5.68}$$

The back-EMF boost ratio and braking torque are controlled by controlling the duty cycle of PWM. Regenerative braking by single-switch strategy can produce enough braking torque in medium to high-speed regions and better capabilities in the recovery of energy.

5.4 Small-signal Analysis of the Converter

The small-signal analysis of the proposed converter using state-space averaging method.The general state space representation of a system is given by:

$$\dot{x}(t) = Ax(t) + Bu(t) \tag{5.69}$$

$$y(t) = Cx(t) + Du(t) \tag{5.70}$$

The state equations of the converter in step-up Mode I operation in CCM are written as:

$$\frac{di_{L1}}{dt} = \frac{V_c L_m}{L} - \frac{L_m V_{co}}{L} + \frac{V_s(L_2 + L_m)}{L} \tag{5.71}$$

$$\frac{di_{L2}}{dt} = \frac{-V_c(L_1 + L_m)}{L} + \frac{V_{co}(L_1 + L_m)}{L} - \frac{V_s L_m}{L} \tag{5.72}$$

$$\frac{dV_c}{dt} = \frac{i_{L2}}{C_1} \tag{5.73}$$

$$\frac{dV_{co}}{dt} = \frac{i_{L2}}{C_o} - \frac{V_{co}}{R_o C_o} \tag{5.74}$$

$$V_o = V_{co} \tag{5.75}$$

The above equation is rewritten in the form of state space as follow:

$$\dot{x}(t) = A_1 x(t) + B_1 u(t) \tag{5.76}$$

$$\begin{pmatrix} \dot{i_{L1}} \\ \dot{i_{L2}} \\ \dot{v_c} \\ \dot{v_{co}} \end{pmatrix} = \begin{pmatrix} 0 & 0 & \frac{L_m}{L} & \frac{-L_m}{L} \\ 0 & 0 & \frac{-(L_1+L_m)}{L} & \frac{(L_1+L_m)}{L} \\ 0 & \frac{1}{C_1} & 0 & 0 \\ 0 & \frac{1}{C_o} & 0 & \frac{-1}{R_o C_o} \end{pmatrix} \begin{pmatrix} i_{L1} \\ i_{L2} \\ v_c \\ v_{co} \end{pmatrix} + \begin{pmatrix} \frac{L_2+L_m}{L} \\ \frac{-L_m}{L} \\ 0 \\ 0 \end{pmatrix} \begin{pmatrix} v_s \end{pmatrix} \tag{5.77}$$

$$y(t) = C_1 x(t) + D_1 u(t) \tag{5.78}$$

$$\begin{pmatrix} v_o \end{pmatrix} = \begin{pmatrix} 0 & 0 & 0 & 1 \end{pmatrix} \begin{pmatrix} i_{L1} \\ i_{L2} \\ v_c \\ v_{co} \end{pmatrix} + \begin{pmatrix} 0 \end{pmatrix} \begin{pmatrix} v_o \end{pmatrix} \tag{5.79}$$

The state equations of the converter in step-up Mode II operation in CCM are written as:

$$\frac{di_{L1}}{dt} = \frac{V_c(L_2+2L_m)}{L} - \frac{V_{co}(L_2+L_m)}{L} + \frac{V_s(L_2+L_m)}{L} \tag{5.80}$$

$$\frac{di_{L2}}{dt} = -\frac{V_c(L_1+2L_m)}{L} + \frac{V_{co}(L_m)}{L} - \frac{V_s L_m}{L} \tag{5.81}$$

$$\frac{dV_c}{dt} = -\frac{IL1}{C_1} + \frac{i_{L2}}{C_1} \tag{5.82}$$

$$\frac{dV_{co}}{dt} = \frac{i_{L1}}{C_o} - \frac{V_{co}}{R_o C_o} \tag{5.83}$$

$$V_o = V_{co} \tag{5.84}$$

The above equation is rewritten in the form of state space as follow:

$$\dot{x}(t) = A_2 x(t) + B_2 u(t) \tag{5.85}$$

$$\begin{pmatrix} \dot{i_{L1}} \\ \dot{i_{L2}} \\ \dot{v_c} \\ \dot{v_{co}} \end{pmatrix} = \begin{pmatrix} 0 & 0 & \frac{L_2+2L_m}{L} & \frac{-(L_2+L_m)}{L} \\ 0 & 0 & \frac{-(L_1+2L_m)}{L} & \frac{L_m}{L} \\ \frac{-1}{C_1} & \frac{1}{C_1} & 0 & 0 \\ \frac{1}{C_o} & 0 & 0 & \frac{-1}{R_o C_o} \end{pmatrix} \begin{pmatrix} i_{L1} \\ i_{L2} \\ v_c \\ v_{co} \end{pmatrix} + \begin{pmatrix} \frac{L_2+L_m}{L} \\ \frac{-L_m}{L} \\ 0 \\ 0 \end{pmatrix} \begin{pmatrix} v_s \end{pmatrix} \tag{5.86}$$

$$y(t) = C_2 x(t) + D_2 u(t) \tag{5.87}$$

$$\begin{pmatrix} v_o \end{pmatrix} = \begin{pmatrix} 0 & 0 & 0 & 1 \end{pmatrix} \begin{pmatrix} i_{L1} \\ i_{L2} \\ v_c \\ v_{co} \end{pmatrix} + \begin{pmatrix} 0 \end{pmatrix} \begin{pmatrix} v_o \end{pmatrix} \tag{5.88}$$

By using state-space averaging technique, A, B, C, D matrix is obtained as:

$$A = A_1 D + A_2(1-D) \tag{5.89}$$

$$B = B_1 D + B_2(1-D) \tag{5.90}$$

$$A = \begin{pmatrix} 0 & 0 & \frac{L_m+(1-D)L_2}{L} & \frac{-(L_m+(1-D)L_2)}{L} \\ 0 & 0 & \frac{-(L_1+L_m(2-D))}{L} & \frac{DL_1+L_m}{L} \\ \frac{-(1-D)}{C_1} & \frac{1}{C_1} & 0 & 0 \\ \frac{(1-D)}{C_o} & \frac{D}{C_o} & 0 & \frac{-1}{R_o C_o} \end{pmatrix} \tag{5.91}$$

$$B = \begin{pmatrix} \frac{L_2+L_m}{L} \\ \frac{-L_m}{L} \\ 0 \\ 0 \end{pmatrix} \tag{5.92}$$

$$C = \begin{pmatrix} 0 & 0 & 0 & 1 \end{pmatrix} \tag{5.93}$$

$$D = \begin{pmatrix} 0 \end{pmatrix} \tag{5.94}$$

Small signal model is derived by applying perturbations, the overall state and output equation of the converter is obtained as:

$$\begin{pmatrix} \widetilde{i_{L1}} \\ \widetilde{i_{L2}} \\ \widetilde{v_c} \\ \widetilde{v_{co}} \end{pmatrix} = \begin{pmatrix} 0 & 0 & \frac{L_m+(1-D)L_2}{L} & \frac{-(L_m+(1-D)L_2)}{L} \\ 0 & 0 & \frac{-(L_1+L_m(2-D))}{L} & \frac{DL_1+L_m}{L} \\ \frac{-(1-D)}{C_1} & \frac{1}{C_1} & 0 & 0 \\ \frac{(1-D)}{C_o} & \frac{(D)}{C_o} & 0 & \frac{-1}{R_oC_o} \end{pmatrix} \begin{pmatrix} \widetilde{i_{L1}} \\ \widetilde{i_{L2}} \\ \widetilde{v_c} \\ \widetilde{v_{co}} \end{pmatrix} + \begin{pmatrix} \frac{v_{co}L_2-v_cL_2}{L} & \frac{L_2+L_m}{L} \\ \frac{v_cL_1+v_{co}L_1}{L} & \frac{-L_m}{L} \\ \frac{i_{L1}}{C_1} & 0 \\ \frac{(i_{L2}-i_{L1})}{C_o} & 0 \end{pmatrix} \begin{pmatrix} \widetilde{d} \\ \widetilde{v_s} \end{pmatrix} \tag{5.95}$$

After substituting all passive elements value from Table 5.1 and duty cycle D = 0.51, control to output transfer function $G_d(s)$ is obtained as follows:

$$G_d(s) = \frac{\widetilde{v_o(s)}}{\widetilde{d(s)}} = \frac{-4.017 \times 10^4 s^3 + 5.78 \times 10^8 s^2 - 5.66 \times 10^{12} s + 6.4 \times 10^{16}}{1.48s^4 + 0.86 \times 10^2 s^3 + 4 \times 10^8 s^2 + 1.18 \times 10^{10} s + 7.84 \times 10^{13}} \tag{5.96}$$

From the above transfer function, it is observed that the all the poles and two zeros lies on left half and one zero lies on right half of S-plane of in root locus. Transfer function of a PI controller is

$$G_{PI} = \frac{K_p s + K_i}{s} \tag{5.97}$$

Ziegler-Nicolous' closed loop method is used to tune the PI controller, the value of K_p = 8 × 10^{-4} and K_i = 0.02 substituted in (5.97) and therefore the closed loop transfer function (CLTF) of the converter is obtained as follows

$$CLTF = \frac{\widetilde{v_o(s)}}{\widetilde{d(s)}} = \frac{-40.17s^4 + 5.75 \times 10^5 s^3 - 5.65 \times 10^9 s^2 + 6.38 \times 10^{13} s + 1.28 \times 10^{15}}{s(1.48s^4 + 86s^3 + 2 \times 10^8 s^2 + 1.18 \times 10^{10} s + 7.84 \times 10^{13})} \tag{5.98}$$

The magnitude and phase plot is obtained from CLTF are shown in Figure 5.15.

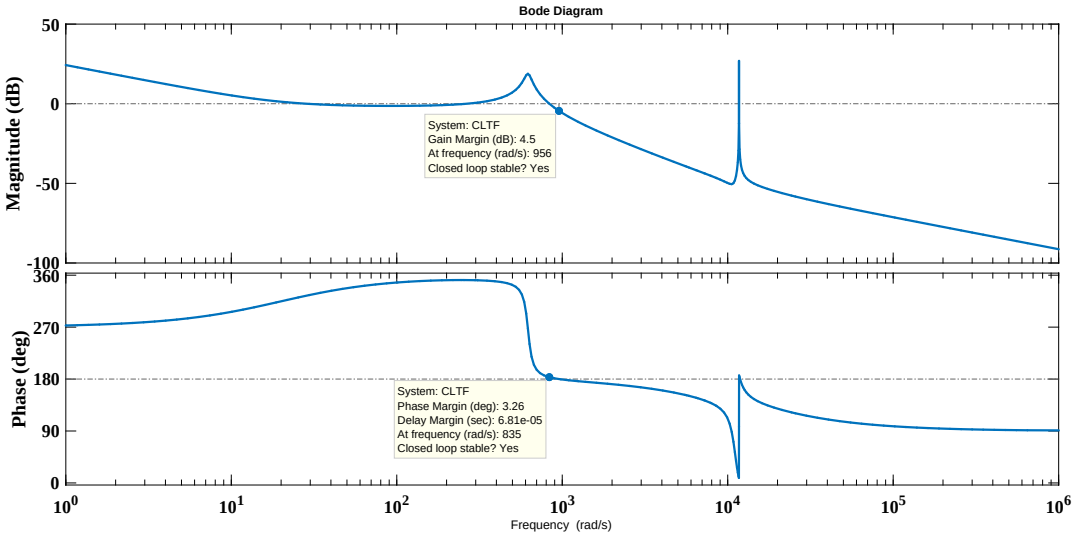

Figure 5.15: Mganitude and phase plot is obtained from CLTF.

5.5 Simulation and Experimental Results

5.5.1 Simulation Results

System at Output Voltage 200 V and Operating Frequency 40 kHz

MATLAB/Simulink is used to the coupled-inductor based QGBC and VSI for the PMBLDC motor in EV application. The PMBLDC motor is coupled with an inertial load through pulley-belt arrangement. The converter with battery voltage V_S= 48 V, output voltage V_o= 200 V, and a switching frequency (f_s) of 40 kHz is simulated. The converter parameters are calculated and listed in Table 5.1 for CCM in step-up and step-down operation.

The switching signal generated for DC-DC converter in step-up operation is shown in Figure 5.16. The switches S_1 and S_2 are switched ON and OFF simultaneously in step-up operation of the converter. The switching signal for PMBLDC motor is generated based on hall sensor signal and it is illustrated in Figure 5.17.

Table 5.1: Converter specifications.

Parameter	Value
Power (P_o)	1 kW
Output voltage (V_o)	200 V
Switching frequency (f_s)	40 kHz
Magnetizing Inductance (L_m)	480 μ H
Leakage inductance (L_1=L_2)	98 μ H
Capacitor (C_s, C_1 C_o)	100 μF 47 μF 200 μF
Switches S_1-S_4	STWA63N65DM2

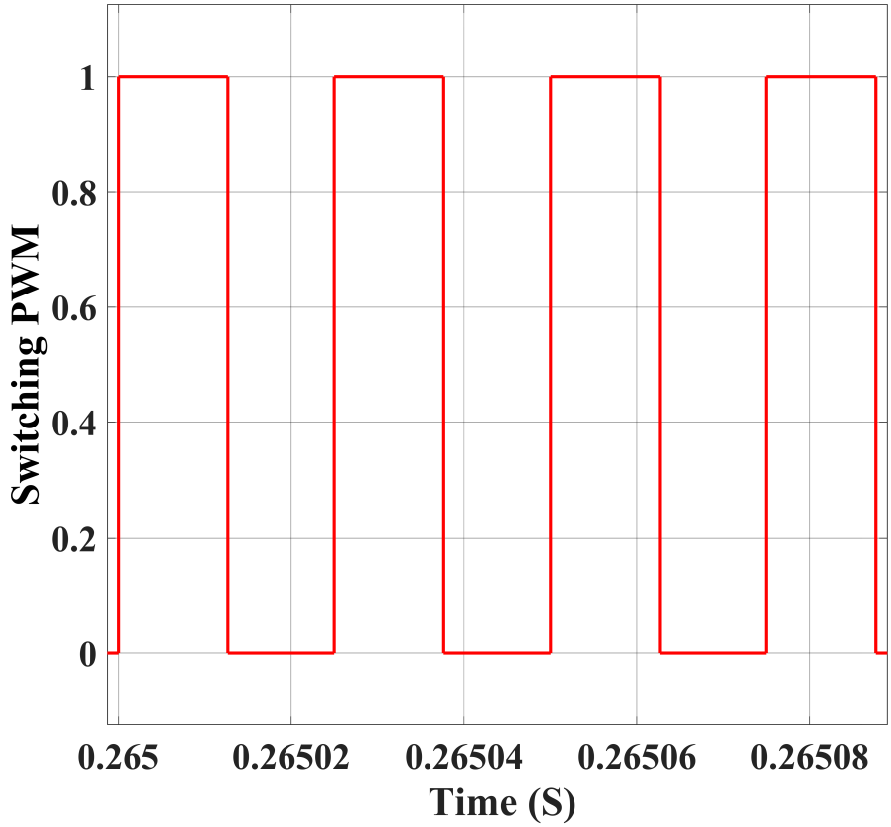

Figure 5.16: Switching PWM for switches S_1 and S_2 during step-up operation of the converter.

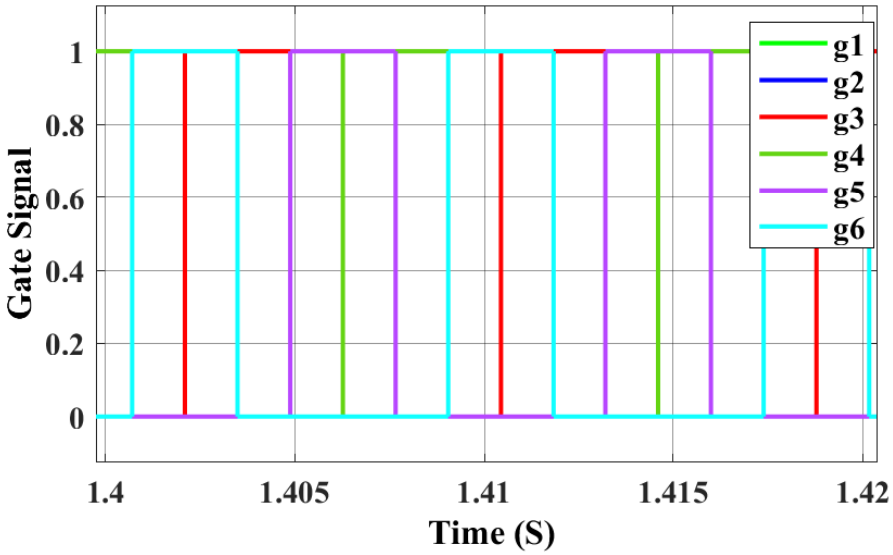

Figure 5.17: Gate signal of voltage source inverter for PMBLDC motor in motoring mode.

The steady-state inductor current I_{L1}, I_{L2} during step-up opertaion of the converter with switching PWM for S_1 and S_2 are illustrated in Figure 5.18. One can see that, when the switch is turned ON, the current in the inductor L_1 decreases while the current in the inductor L_2 increases.

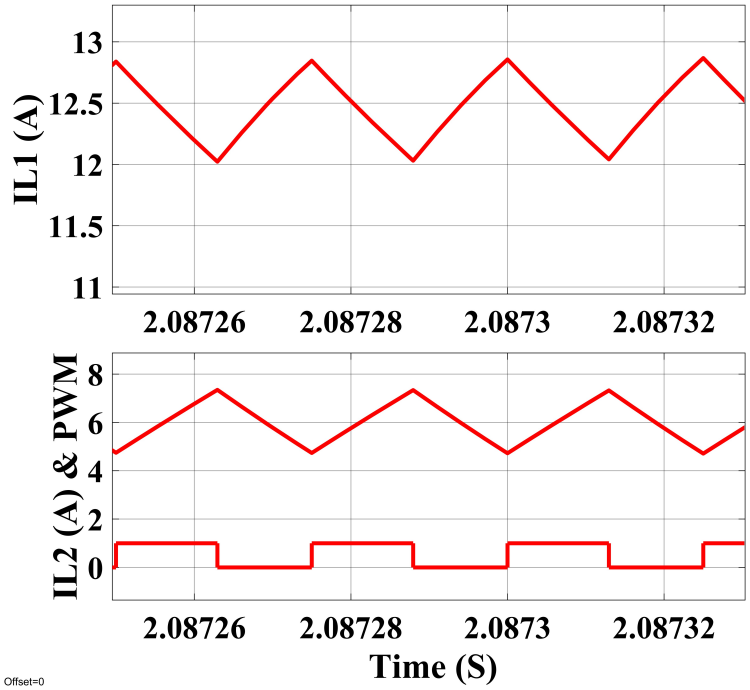

Figure 5.18: Steady-state inductor currents I_{L1}, I_{L2} and switching PWM during step-up operation of the converter.

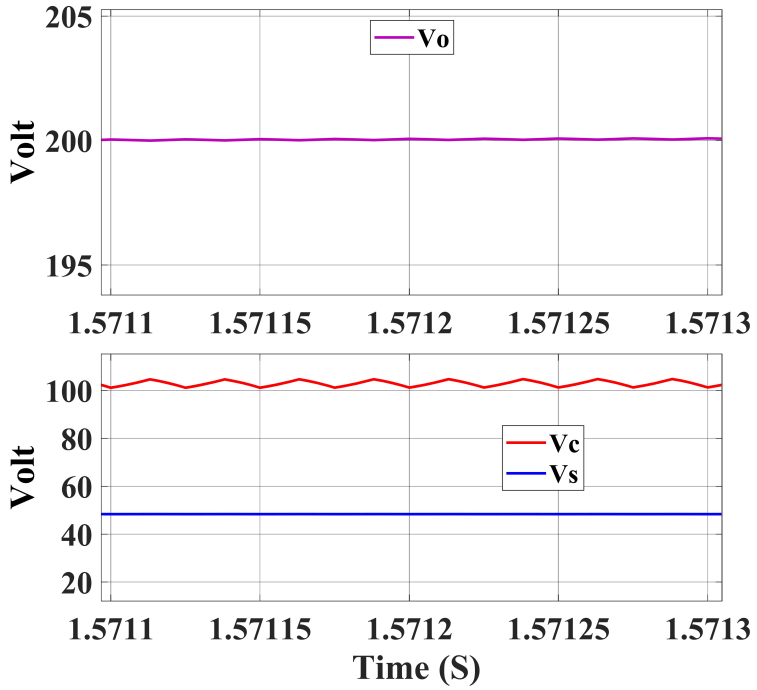

Figure 5.19: Steady-state input and output voltage during step-up operation.

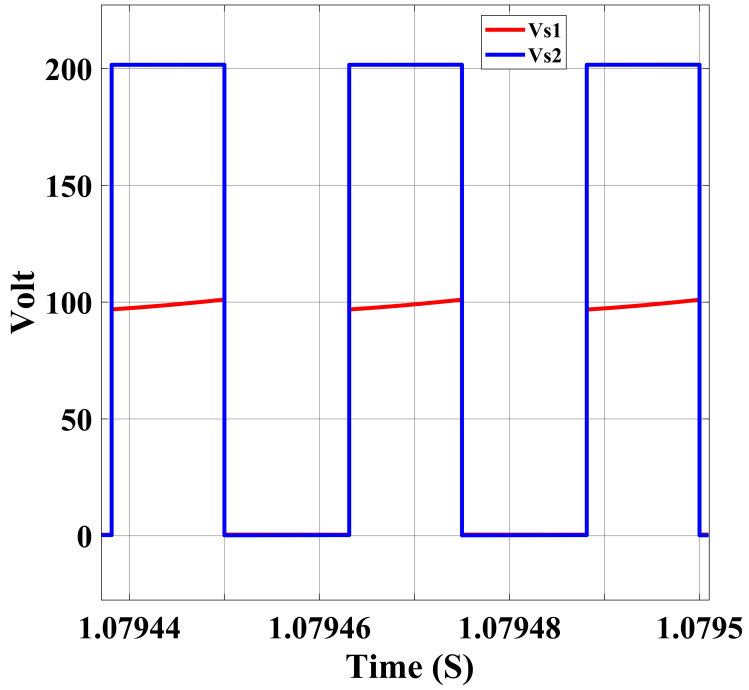

Figure 5.20: Voltage stress on switches S_1 and S_4 during step-up operation of the converter.

Figure 5.20 depicts the voltage stress on switches S_1 and S_4 during the converter's step-up operation. The steady-state output voltage with input voltage during step-up

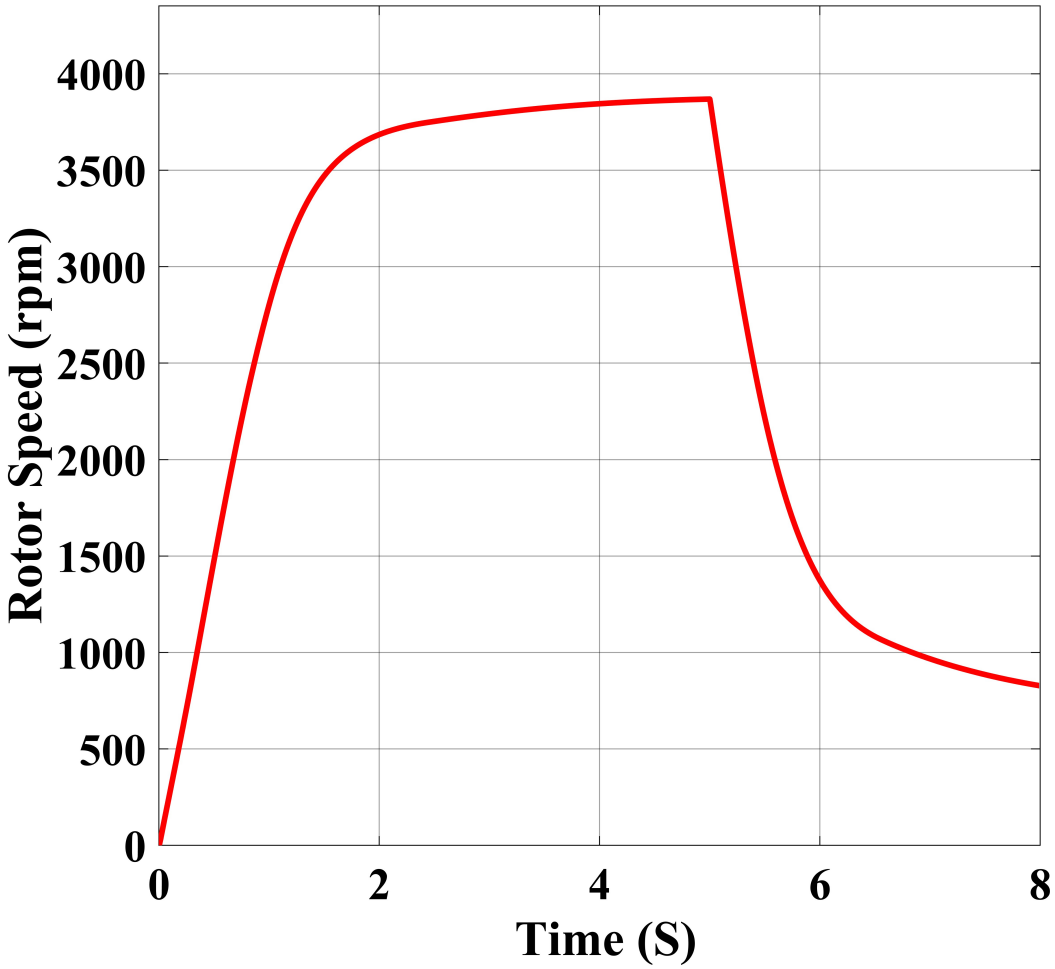

Figure 5.21: Motor speed characteristics.

operation of the converter is illustrated in Figure 5.19. One can see that the output voltage V_o= 200 V with input voltage V_s= 48 V and capacitor voltage V_c= 102 V in the Figure 5.19. When regenerative braking is applied, the PMBLDC motor acts as a generator, and the motor's back-EMF is enhanced to extract the maximum energy stored in the inertial flywheel even at low rotor speed, which is then sent back to the battery by stepping down the voltage to battery level voltage. The proposed converter operates in step-down mode during RB. The speed characteristic of the PMBLDC motor is shown in Figure 5.21. The MATLAB/Simulation is run for 8s. The motoring operation from 0s to 5s speed of motor reaches around 3600 rpm and at 5s RB is applied then speed decrease around 800 rpm at 8s which is illustrated in Figure 5.21.

System at Output Voltage 98 V and Operating Frequency 15 kHz

MATLAB/Simulink is used to the coupled-inductor based QGBC and VSI for the PMBLDC motor in EV application. The PMBLDC motor is coupled with an inertial load through pulley-belt arrangement. The converter with battery voltage V_S= 48 V, output voltage V_o= 98 V, and a switching frequency (f_s) of 15 kHz is simulated. The converter parameters are calculated and listed in Table 5.2 for CCM in step-up and step-down operation. The steady-state output voltage V_o, capacitor voltage V_c and input voltage V_s during

Table 5.2: Converter specifications.

Parameter	Value
Power (P_o)	1 kW
Output voltage (V_o)	98 V
Switching frequency (f_s)	15 kHz
Magnetizing Inductance (L_m)	1.1 mH
Leakage inductance (L_1=L_2)	220 μ H
Capacitor (C_s, C_1 C_o)	100 μF 47 μF 200 μF
Switches S_1-S_4	STWA63N65DM2

step-up operation are illustrated in Figure 5.22. The steady-state inductor current I_{L1}, I_{L2} during step-up opertaion of the converter with switching PWM are shown in Figure 5.23.

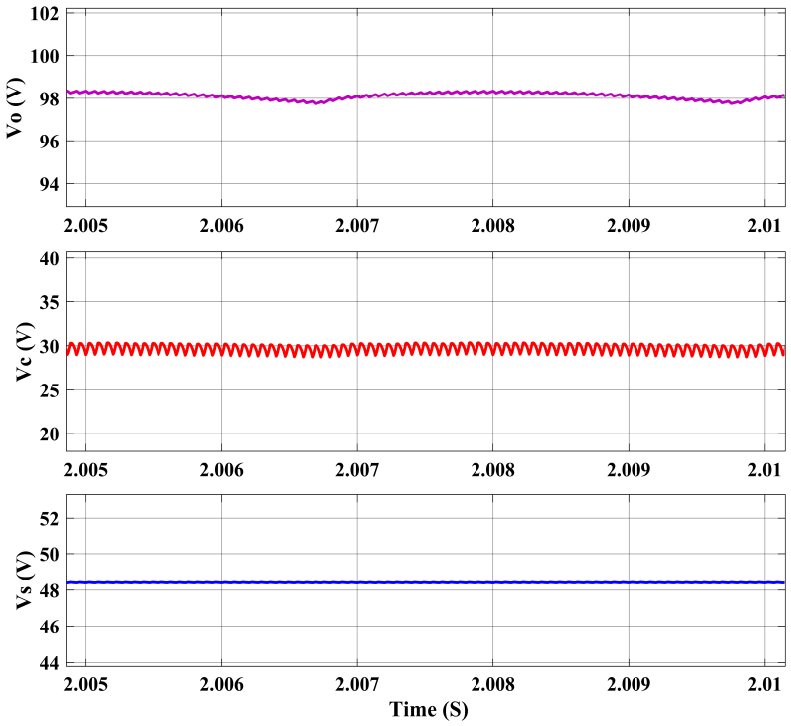

Figure 5.22: Output voltage V_o, capacitor voltage V_c and input voltage V_s during step-up operation.

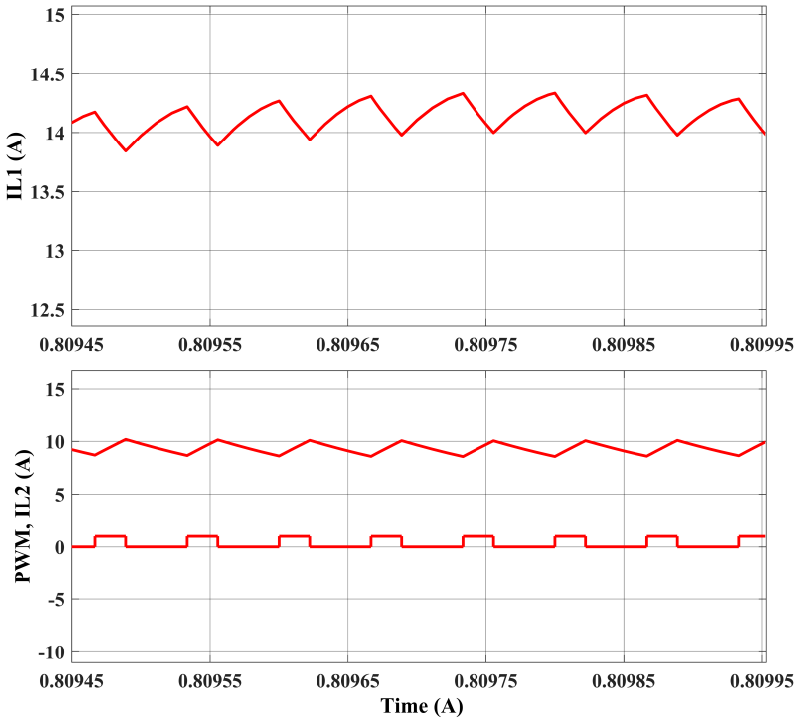

Figure 5.23: Steady-state inductor currents I_{L1}, I_{L2} and switching PWM during step-up operation.

The voltage stress on switches S_1 and S_2 during the converter's step-up operation are depicted in Figure 5.24.

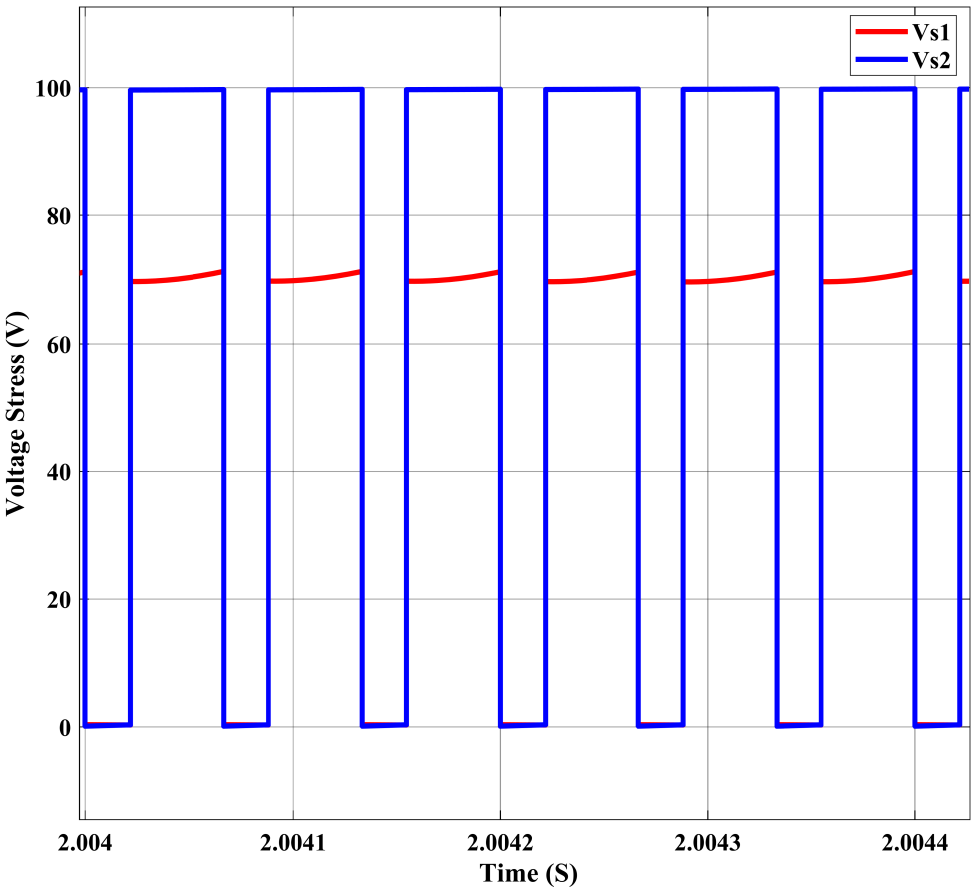

Figure 5.24: Voltage stress on switches S_1 and S_2 during step-up operation of the converter.

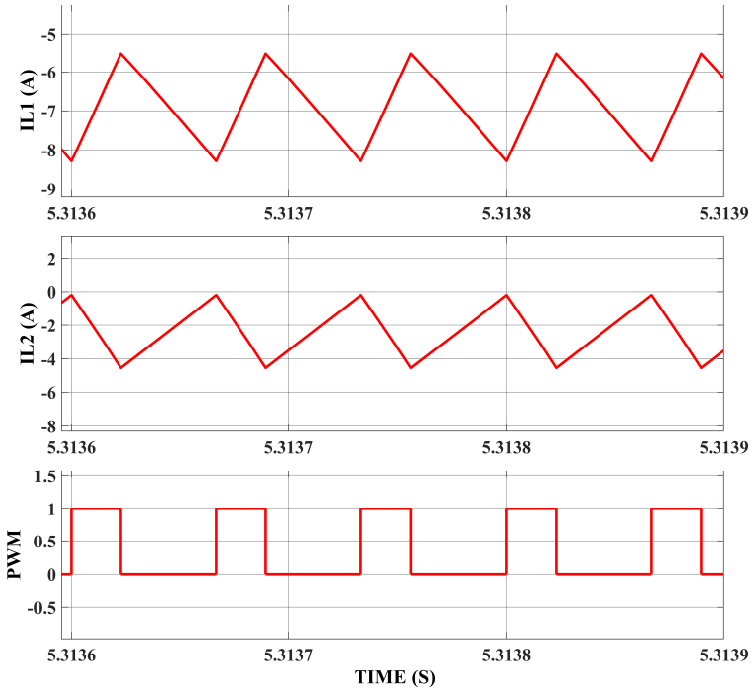

Figure 5.25: Inductor current I_{L1}, I_{L2} with switching PWM during step-down operation of the converter.

The steady-state inductor current I_{L1}, I_{L2} with switching PWM during step-down operation of the converter are illustrated in Figure 5.25.

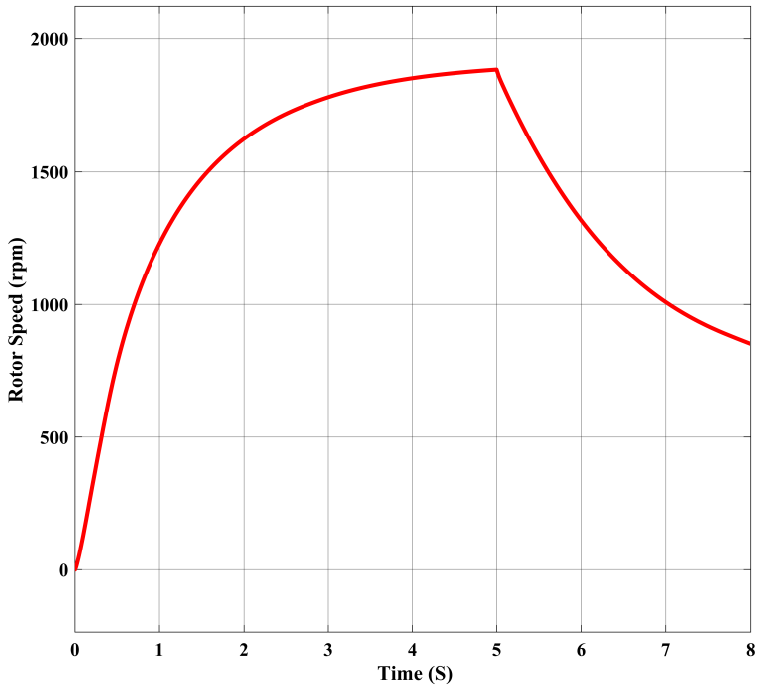

Figure 5.26: PMBLDC motor speed characteristics.

The simulation run for t=8s, during 0s to 5s motoring mode and at t=5s regenerative braking is applied the speed start reducing from 5s to 8s. The PMBLDC motor speed characteristics is illustrated in Figure 5.26.

5.5.2 Experimental Results

System at Output Voltage 200 V and operating frequency 40 kHz

The converter prototype is being designed and developed in the lab for experimental validation. The hardware setup of the converter is shown in Figure 5.27.

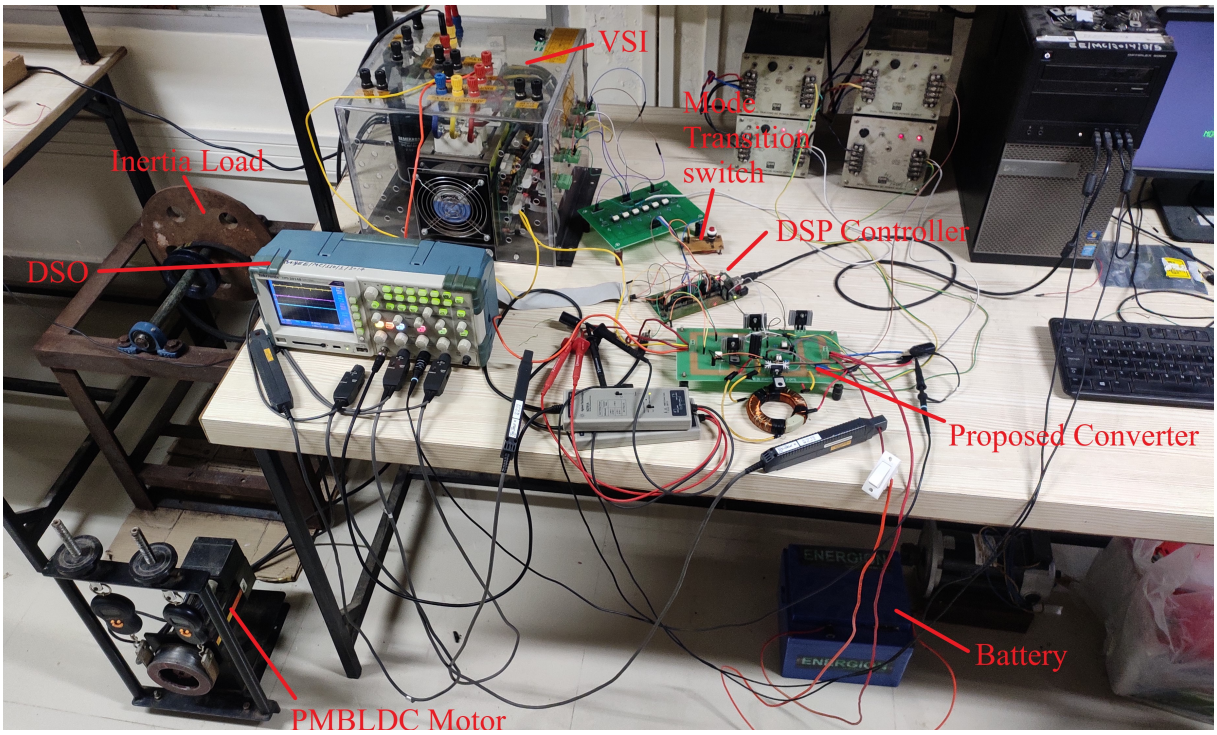

Figure 5.27: Experimental setup.

The Lithium-ion battery is connected to the converter's input, the converter's output is connected to the VSI, the PMBLDC motor is connected to the VSI and a pulley belt arrangement. The TMS320F28335 DSP controller generates the PWM signal for the converter and VSI. During the step-up operation of the converter, the load torque is applied through the belt on the pulley. In step-up operation, Figure 5.28 illustrates the steady-state output voltage V_o, battery voltage V_s, inductor current I_{L1} and inductor current I_{L2}. One can see that the input current ripple is minimum and the output voltage is at 200 V.

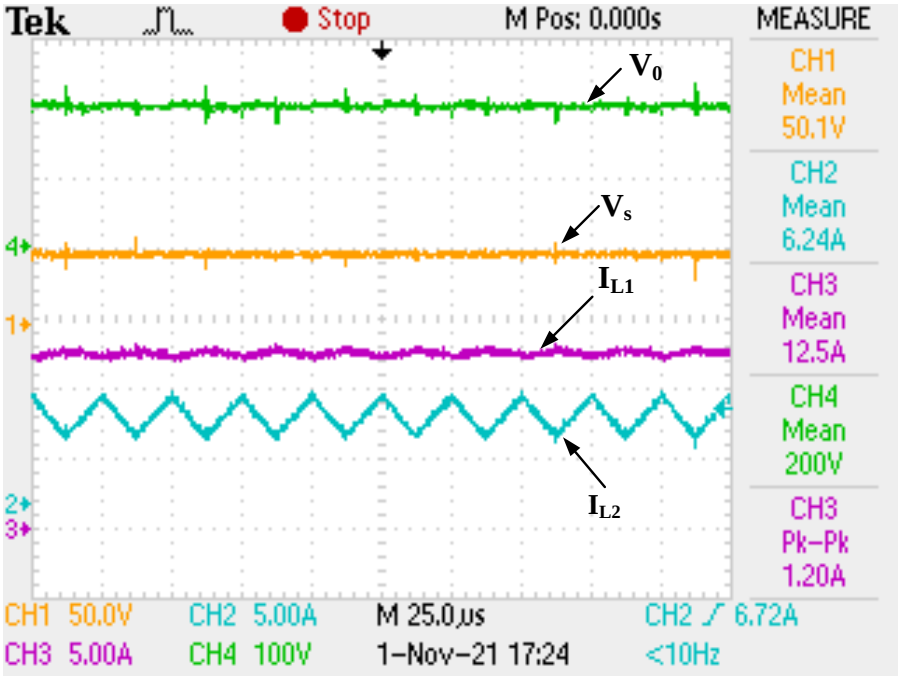

Figure 5.28: Steady-state output voltage V_o, input voltage V_s, inductor current I_{L1}, and inductor current I_{L2} in step-up operation.

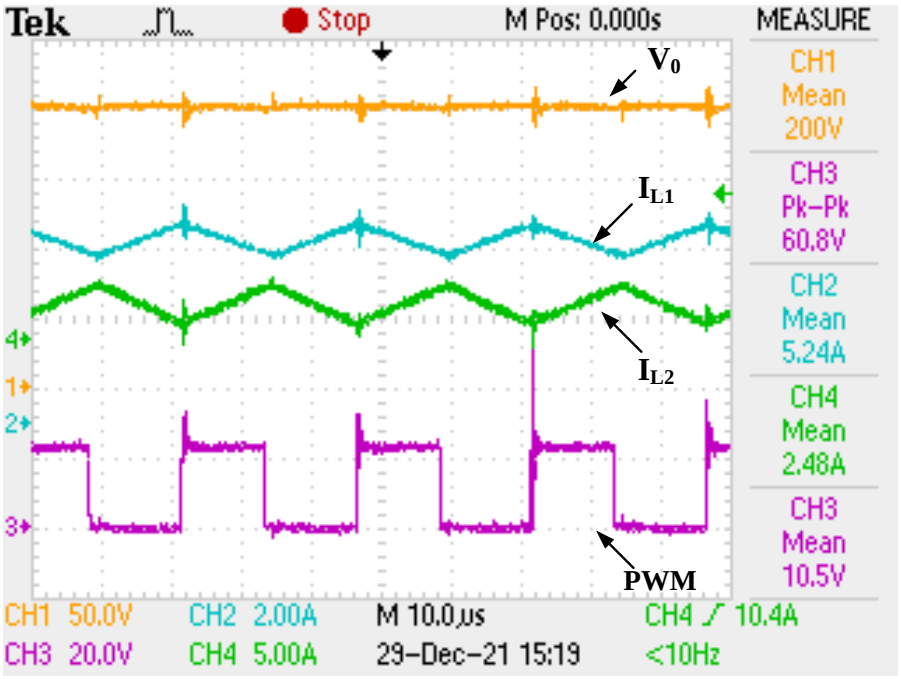

Figure 5.29: Output voltage V_o, inductor current I_{L1}, inductor current I_{L2}, and switching PWM of switch in step-up operation.

The output voltage, inductor currents, and switching PWM of switches S_1 and S_2

are shown in Figure 5.29. One can see that in Figure 5.29 when switches S_1 and S_2 are turned ON, the inductor current I_{L1} decrease and the inductor current I_{L2} increase.

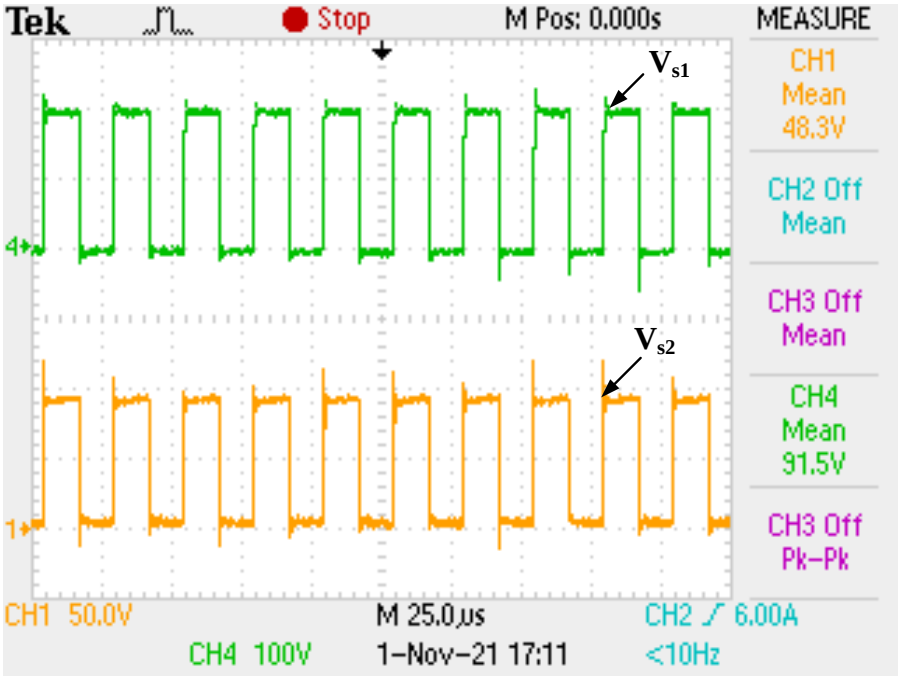

Figure 5.30: The voltage stress on switches S_1 and S_2 during step-up operation of the converter.

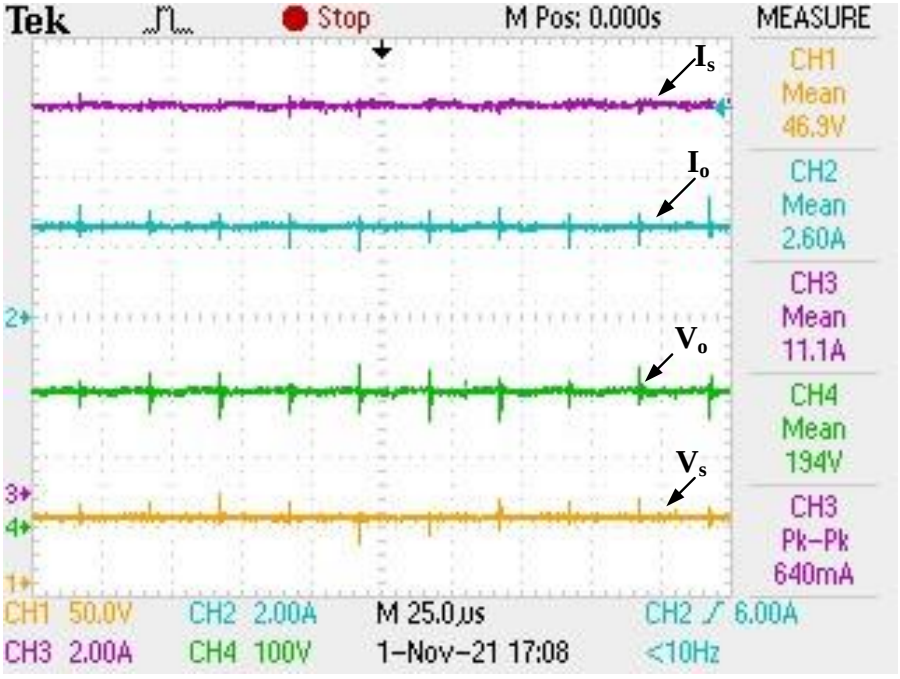

Figure 5.31: The steady-state output voltage V_o, output current I_o, input voltage V_s, and input current I_s in step-up operation of the converter.

The voltage stress on switches S_1 and S_2 during step-up operation of the converter are shown in Figure 5.30. The maximum voltage stress on switch S_1 and S_3 are the same and it is equal to 100 V during step-up operation of the converter as shown in Figure 5.30. The maximum voltage stress on switch S_2 and S_4 are the same and it is equal to 200 V during step-up operation of the converter as shown in Figure 5.30. The converter's steady-state output voltage, output current, input voltage, and input current during step-up operation are shown in Figure 5.31.

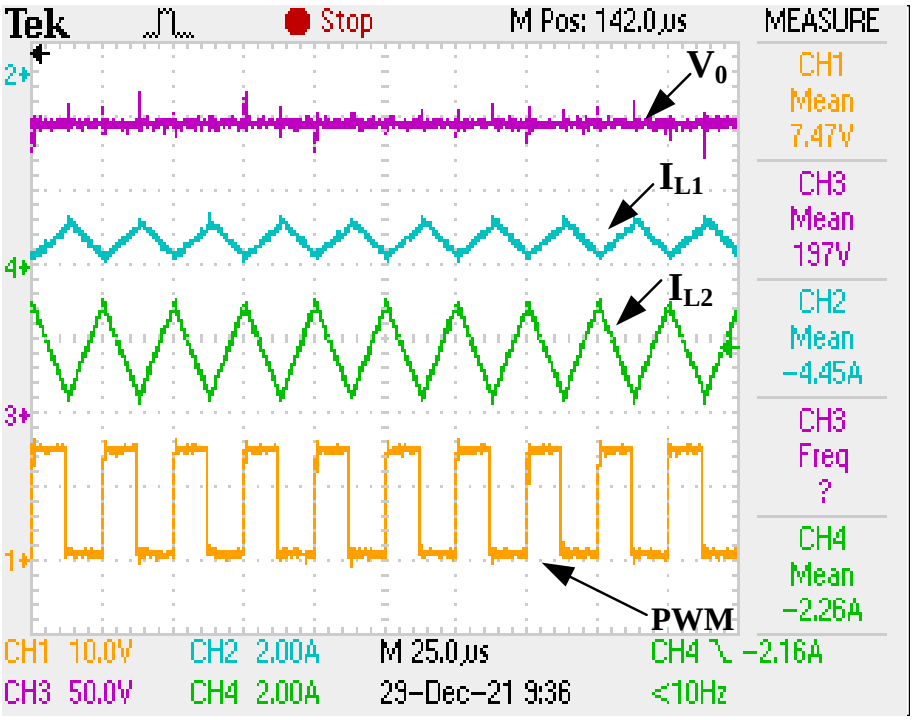

Figure 5.32: Steady-state output voltage V_o, inductor currents I_{L1}, and I_{L2} with switching PWM during step-down operation.

The PMBLDC motor is coupled with an inertial load through the belt to demonstrate RB functioning. When RB is applied, the PMBLDC motor acts as a generator, extracting energy from the stored kinetic energy in the inertial load and feeding it back to the battery via the converter, which steps down the voltage to battery level. The converter will operate as a step-down during RB of PMBLDC motor. Figure 5.32 depicts the steady-state inductor currents and output voltage with switching PWM during regenerative braking. When switches S_3 and S_4 are turned ON, the inductor current I_{L1} decreases, the inductor current I_{L2} increases, and when OFF I_{L1} increases, I_{L2} decreases.

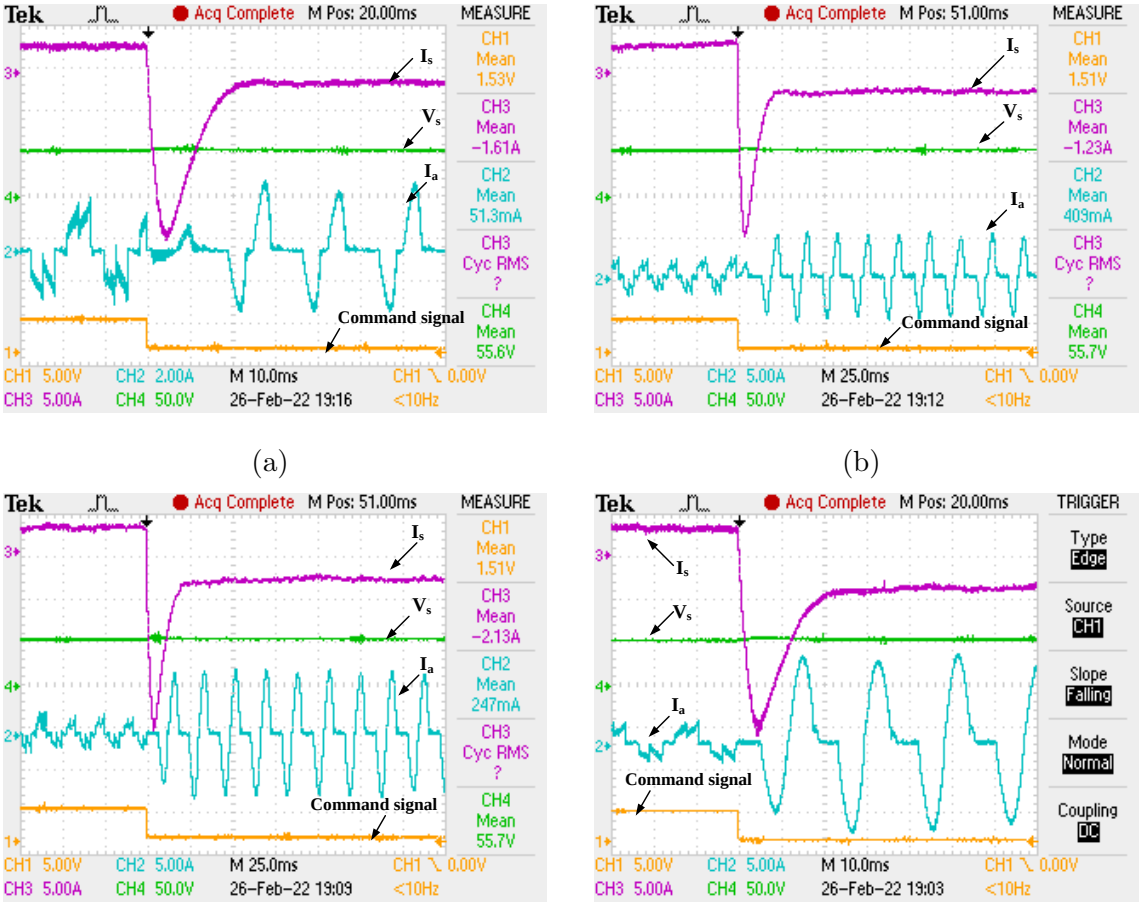

Figure 5.33: Armature current, battery current, battey voltage, command signal at different braking duty (a) $\delta = 0.4$ (b) $\delta = 0.5$ (c) $\delta = 0.6$ and (d) $\delta = 0.7$.

The single-switch control strategy of VSI for RB of PMBLDC motor is done at different braking duties. The braking duty is varied from 0.4 to 0.7, the armature current, battery current, battery voltage, and command signal for RB action is illustrated in Figure 5.33. When the command signal is high, the PMBLDC motor acts in motoring operation and when the command signal goes low, the PMBLDC motor act as a generator in RB. One can see that as braking duty increases then the armature current, battery charging current.

System at Output Voltage 98 V and Operating Frequency 15 kHz

The converter prototype is being designed and developed in the lab for experimental validation. The hardware setup of the converter is shown in Figure 5.27. During the step-up operation of the converter, the load torque is applied through the belt on the

pulley. The steady-state output voltage (V_o), capacitor voltage (V_c), input current (I_s) and input voltage (V_s) during step-up operation of converter are shown n Figure 5.34. One can see that V_o= 98.8 V, V_c= 29.9 V, I_s= 7.71 A and V_s= 50 V at some load.

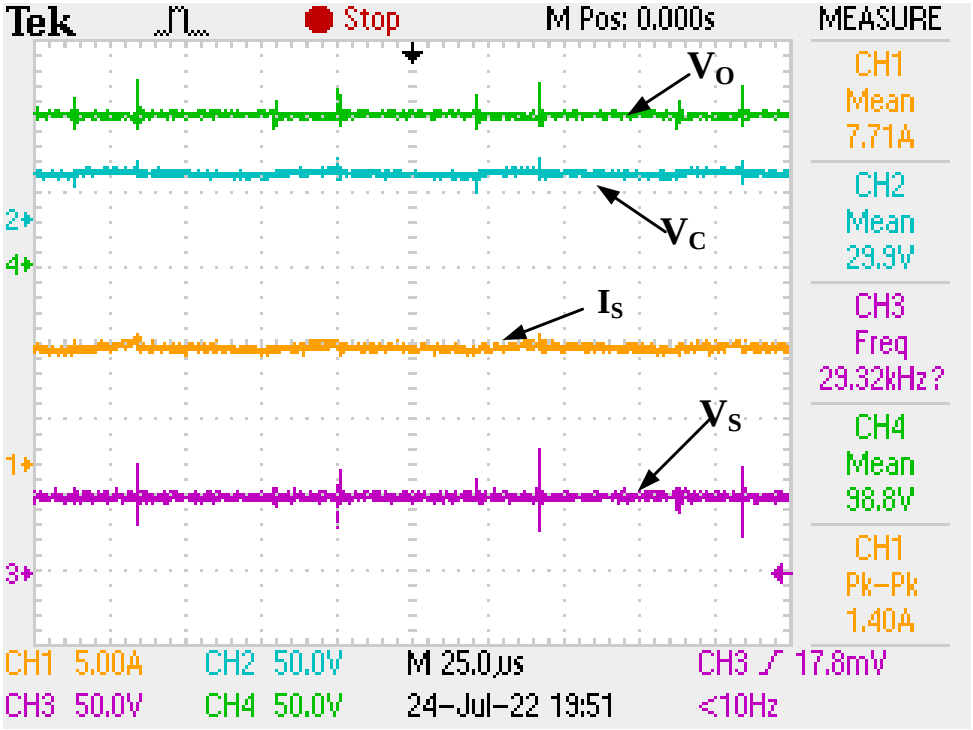

Figure 5.34: Output voltage (V_o), capacitor voltage (V_c), input current (I_s) and input voltage (V_s) during step-up operation converter.

The inductor current I_{L1}, I_{L2}, output voltage V_o with switching PWM during step-up mode are illustrated in Figure 5.35. The voltage stress on switches S_1, S_2, output voltage and input current are shown in Figure 5.36 in step-up operation of converter.

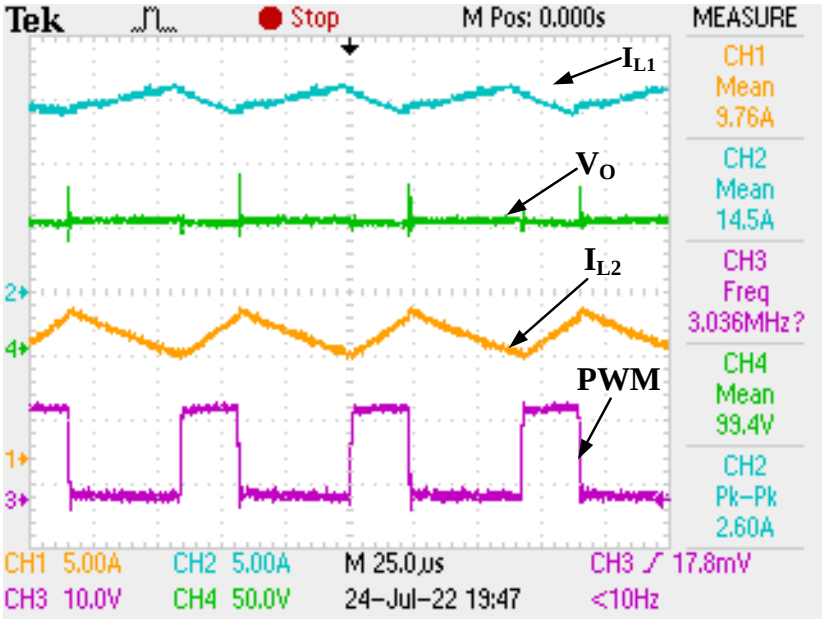

Figure 5.35: The inductor current I_{L1}, I_{L2}, output voltage V_o with switching PWM during step-up operation pf converter.

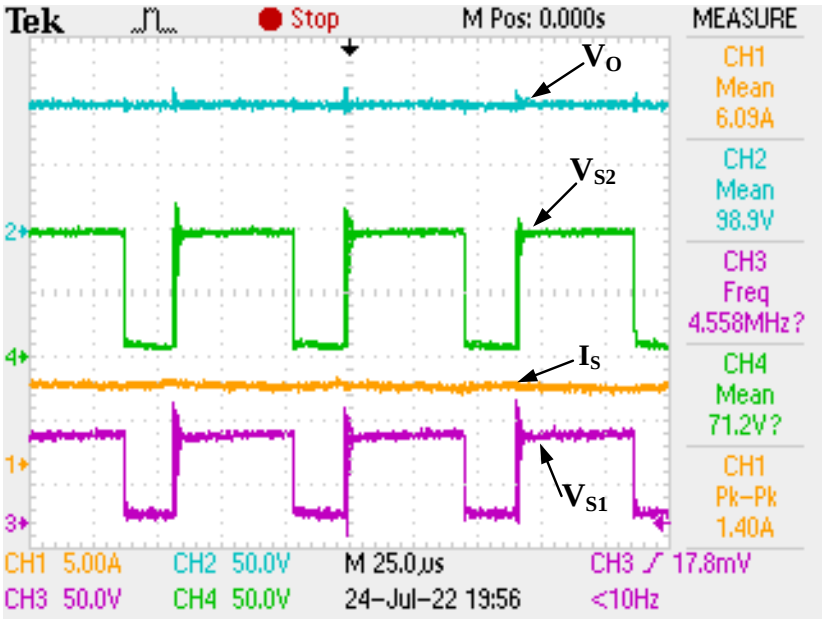

Figure 5.36: The voltage stress on switches S_1, S_2, output voltage and input current during step-up operation of converter.

The steady-state inductor currents (I_{L1}, I_{L2}) and output voltage with switching PWM during regenerative braking or step-down operation of converter are depicted in Figure 5.37.

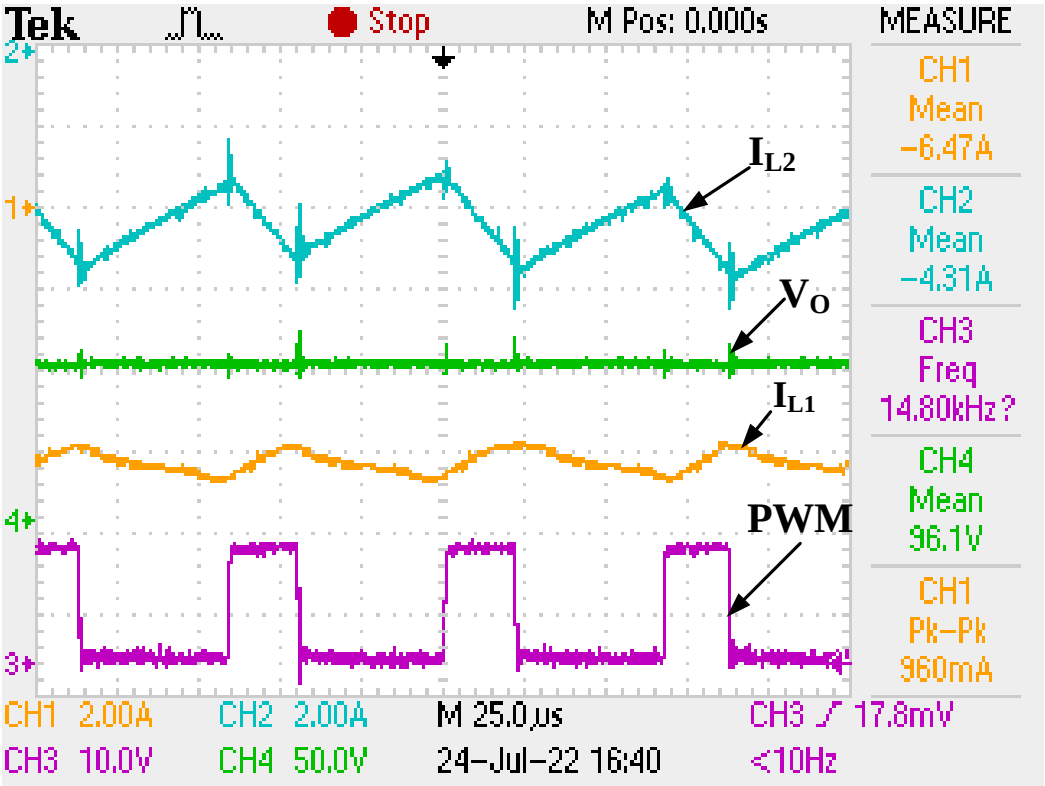

Figure 5.37: Inductor currents I_{L1}, I_{L2} and output voltage with switching PWM during regenerative braking or step-down operation of converter.

The PMBLDC motor is coupled with an inertial load through the belt to demonstrate RB functioning. When RB is applied, the PMBLDC motor acts as a generator, extracting energy from the stored kinetic energy in the inertial load and feeding it back to the battery via the converter, which steps down the voltage to battery level. The converter will operate as a step-down during RB of PMBLDC motor.

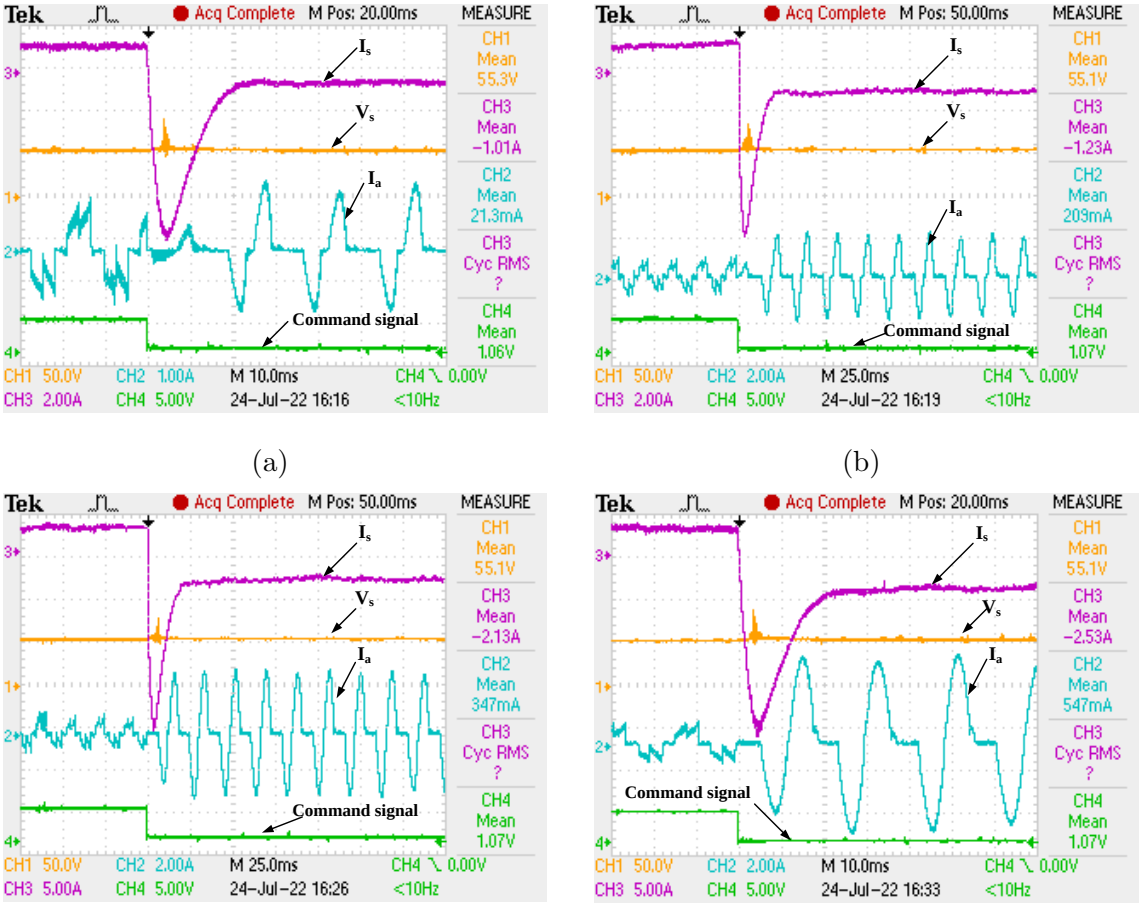

Figure 5.38: Armature current, battery current, battey voltage, command signal at different braking duty (a) $\delta = 0.4$ (b) $\delta = 0.5$ (c) $\delta = 0.6$ and (d) $\delta = 0.7$.

The single-switch control strategy of VSI for RB of PMBLDC motor is done at different braking duties. The braking duty is varied from 0.4 to 0.7, the armature current, battery current, battery voltage, and command signal for RB action is illustrated in Figure 5.38. When the command signal is high, the PMBLDC motor acts in motoring operation and when the command signal goes low, the PMBLDC motor act as a generator in RB. One can see that as braking duty increases then the armature current, battery charging current.

Figure 5.39 depicts the converter's efficiency curve in step-up operations at two different output voltage anf operating frequency. One can see that in step-up operation the maximum efficiency is 95 % for output voltage 200 V and frequency of 40 kHz. The othe curve attend maximum efficiency is 96 % for output voltage 98 V and frequency of 15 kHz.

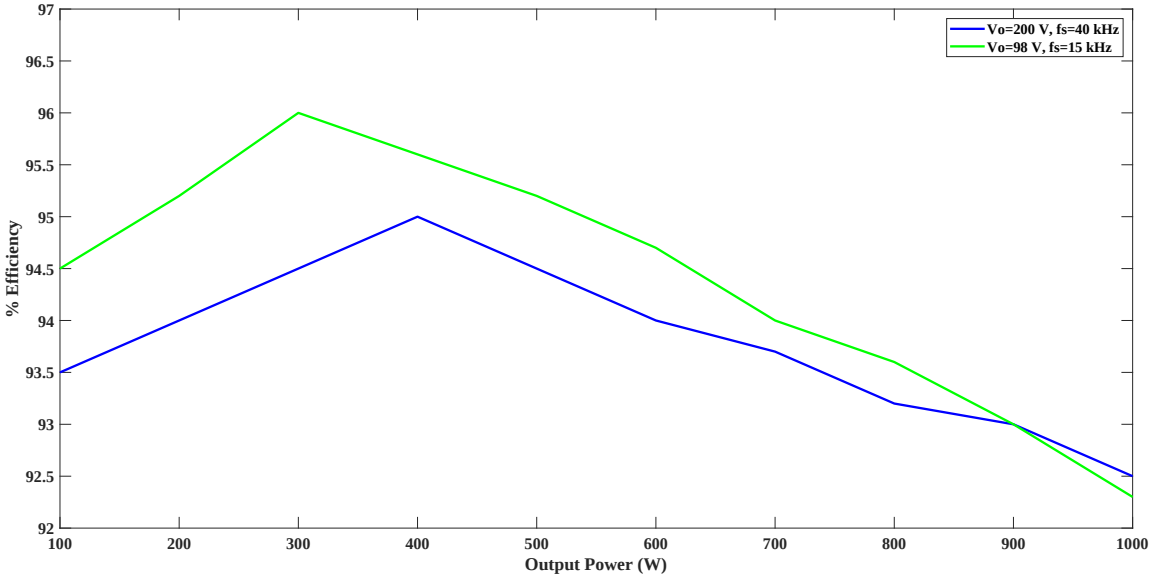

Figure 5.39: The efficiency curve of the converter in step-up operation.

The results obtained in experimental is compared with simulation results at two different output voltage and frequency for validation for validation are done in Table 5.3 and 5.4. The speed of the motor during experiment is measured with stroboscope tachometer.

Table 5.3: Comparison of simulation and experimental results for output voltage 200 V and operating frequency 40 kHz.

Parameters	Output Voltage V_o	Input current I_i	Inductor current	Input current ripple	Voltage stress	Motor speed
Simulation	200 V	12.3 A	I_{L1}=12.3 A I_{L2}=6 A	7 %	V_{s1}=V_{s3}=102 V V_{s2}=V_{s4}=200 V	3600 rpm
Experimental	200 V	12.5 A	I_{L1}=12.5 A I_{L2}=6.25 A	10 %	V_{s1}=104 V V_{s2}=206 V	3500 rpm

The comparison of different bidirectional DC DC converters with the proposed converter is done in Table 5.5.

Table 5.4: Comparison of simulation and experimental results for output voltage 98 V and operating frequency 15 kHz.

Parameters	Output Voltage V_o	Input current I_i	Inductor current	Input current ripple	Voltage stress	Motor speed
Simulation	98 V	14 A	I_{L1}=14 A I_{L2}=9 A	30 %	V_{s1}=V_{s3}=69 V V_{s2}=V_{s4}=98 V	1800 rpm
Experimental	99.4 V	14.5 A	I_{L1}=14.5 A I_{L2}=9.76 A	30%	V_{s1}=72 V V_{s2}=100 V	1750 rpm

Table 5.5: Comparision of different bidirectional converters with proposed converter

Reference	Total components	Voltage ratio boost	Voltage ratio buck	Input current ripple	Maximum Efficiency
Converter in [114]	1 inductor 1 coupled inductor 5 capacitors 4 power switches	$\frac{2+kn}{(1-D)}$	$\frac{D}{2+kn}$	10 %	94 %
Converter in [123]	1 coupled inductor 3 capacitors 4 power switches	$\frac{1+n}{1-D}$	$\frac{(1-D)}{1+n}$	40 %	95 %
Converter in [124]	1 coupled inductor 3 capacitors 4 power switches	$\frac{2+n}{1-D}$	$\frac{D}{2+n}$	50 %	95 %
Proposed converter	1 coupled inductor 2 capacitors 4 power switches	$\frac{1}{(1-D)^2}$	D^2	10 % (40 kHz) 30 % (15 kHz)	95 % (40 kHz) 96 % (15 kHz)

5.6 Conclusion

For an EVapplication, the suggested converter was conceived, developed in the lab, and tested on a PMBLDC motor in motoring and regenerative braking mode. The proposed converter operation for step-up and step-down modes in CCM and DCM was discussed. The voltage gain is found to be similar to that of a cascaded boost converter in step-up mode, whereas it is comparable to that of a cascaded buck converter in step-down

mode. However, the presence of coupled inductor with the appropriate number of turns is exhibiting a lower current ripple in the modified converter. The working of the converter and energy flow direction change in both the step-up and step-down modes are verified by using a mode transition switch. The single-switch control strategy of VSI for RB of PMBLDC motor gives a smooth armature current profile. The proposed converter is found to achieve significant voltage gain with a low current ripple at all operation points. The VSI control approach is used to boost back-EMF of the PMBLDC motor by use of self-inductance.